

AD _____

Award Number: DAMD17-97-1-7320

TITLE: Identification of Markers of the Invasive Phenotype in Human Breast Cancer (96 Cancer)

PRINCIPAL INVESTIGATOR: Peter Watson, M.B.

CONTRACTING ORGANIZATION: University of Manitoba
Winnipeg, Manitoba Canada R3E 0W3

REPORT DATE: October 1999

TYPE OF REPORT: Annual

PREPARED FOR: U.S. Army Medical Research and Materiel Command
Fort Detrick, Maryland 21702-5012

DISTRIBUTION STATEMENT: Approved for public release
distribution unlimited

The views, opinions and/or findings contained in this report are those of the author(s) and should not be construed as an official Department of the Army position, policy or decision unless so designated by other documentation.

DTIC QUALITY INSPECTED 4

20001017 036

REPORT DOCUMENTATION PAGEForm Approved
OMB No. 074-0188

Public reporting burden for this collection of information is estimated to average 1 hour per response, including the time for reviewing instructions, searching existing data sources, gathering and maintaining the data needed, and completing and reviewing this collection of information. Send comments regarding this burden estimate or any other aspect of this collection of information, including suggestions for reducing this burden to Washington Headquarters Services, Directorate for Information Operations and Reports, 1215 Jefferson Davis Highway, Suite 1204, Arlington, VA 22202-4302, and to the Office of Management and Budget, Paperwork Reduction Project (0704-0188), Washington, DC 20503

1. AGENCY USE ONLY (Leave blank)		2. REPORT DATE October 1999	3. REPORT TYPE AND DATES COVERED Annual (01 Sep 98 - 01 Sep 99)	
4. TITLE AND SUBTITLE Identification of Markers of the Invasive Phenotype in Human Breast Cancer (96 Cancer)			5. FUNDING NUMBERS DAMD17-97-1-7320	
6. AUTHOR(S) Peter Watson, M.B.				
7. PERFORMING ORGANIZATION NAME(S) AND ADDRESS(ES) University of Manitoba Winnipeg, Manitoba, R3E 0W3 Canada e-mail: pwatson@cc.umanitoba.ca			8. PERFORMING ORGANIZATION REPORT NUMBER	
9. SPONSORING / MONITORING AGENCY NAME(S) AND ADDRESS(ES) U.S. Army Medical Research and Materiel Command Fort Detrick, Maryland 21702-5012			10. SPONSORING / MONITORING AGENCY REPORT NUMBER	
11. SUPPLEMENTARY NOTES				
12a. DISTRIBUTION / AVAILABILITY STATEMENT Approved for public release distribution unlimited				12b. DISTRIBUTION CODE
13. ABSTRACT (Maximum 200 Words) Our goal is to identify genes involved in the development of the invasive phenotype as these may offer predictive markers and markers of risk of invasive disease in pre-invasive lesions. We have applied our tissue based strategy to directly identify differentially expressed genes between pre-invasive in-situ (DCIS) and adjacent early invasive tumor cell populations and have completed assessment of 5 tumors and identified two promising candidate 'invasion' genes. Psoriasin (S100 A7) has been pursued by assessment of persistent expression in invasive tumors, showing that high levels correlate with ER-ve and node +ve status. The functional role has been pursued by transfection and overexpression in invasive (MDA-MB-231) and pre-neoplastic (MCF10AT) breast cell lines, and yeast 2-hybrid assay to search for interacting proteins. Lumican is a small leucine-rich proteoglycan, overexpressed in stroma adjacent to in-situ elements and at the margin of invasive elements. Lumican has been pursued by detailed study of expression pattern in-vivo and comparison with expression profiles of related proteoglycans. The functional role is being pursued by study of transfection to achieve overexpression in fibroblasts, to assess the effect of this on epithelial cells in in-vitro assays.				
14. SUBJECT TERMS Breast Cancer, Microdissection, Pathology, Subtraction hybridisation, microarray, invasion,				15. NUMBER OF PAGES 93
				16. PRICE CODE
17. SECURITY CLASSIFICATION OF REPORT Unclassified	18. SECURITY CLASSIFICATION OF THIS PAGE Unclassified	19. SECURITY CLASSIFICATION OF ABSTRACT Unclassified	20. LIMITATION OF ABSTRACT Unlimited	

FOREWORD

Opinions, interpretations, conclusions and recommendations are those of the author and are not necessarily endorsed by the U.S. Army.

_____ Where copyrighted material is quoted, permission has been obtained to use such material.

_____ Where material from documents designated for limited distribution is quoted, permission has been obtained to use the material.

_____ Citations of commercial organizations and trade names in this report do not constitute an official Department of Army endorsement or approval of the products or services of these organizations.

_____ In conducting research using animals, the investigator(s) adhered to the "Guide for the Care and Use of Laboratory Animals," prepared by the Committee on Care and use of Laboratory Animals of the Institute of Laboratory Resources, national Research Council (NIH Publication No. 86-23, Revised 1985).

✓ For the protection of human subjects, the investigator(s) adhered to policies of applicable Federal Law 45 CFR 46.

✓ In conducting research utilizing recombinant DNA technology, the investigator(s) adhered to current guidelines promulgated by the National Institutes of Health.

✓ In the conduct of research utilizing recombinant DNA, the investigator(s) adhered to the NIH Guidelines for Research Involving Recombinant DNA Molecules.

_____ In the conduct of research involving hazardous organisms, the investigator(s) adhered to the CDC-NIH Guide for Biosafety in Microbiological and Biomedical Laboratories.

P. H. Lohman 1st Sept '91
PI - Signature Date

TABLE OF CONTENTS

Front cover	1
SF298 Report documentation page	2
Foreword	3
Table of Contents	4
Introduction	5
Body	6-11
Key Research Accomplishments	12
Reportable Outcomes	13
Conclusions	14
References	15-16
Appendixes	17-93

INTRODUCTION.

The management of DCIS depends on the estimation of the likelihood of recurrence as in-situ or invasive disease¹. Recent morphological studies have provided useful potential improvements to older classifications of pre-invasive disease with more accurate prognostic significance, however there is clearly a need for better predictors of biological potential². Advances in our understanding of the genes involved in the critical process of epithelial cell invasion and alterations that occur in these genes in human tumors is likely to yield such predictors³. To address this critical issue in the biology of early breast tumor progression, many groups have surveyed DCIS lesions with microsatellite markers in search of regions of DNA that may harbor tumor invasion suppressor genes⁴. This approach has yielded some interesting loci but not specific genes as yet. We have undertaken an alternative novel approach in our laboratory to identify genes and alterations that may contribute to the invasive phenotype in-vivo. This approach has required technical development to enable microdissection of histologically defined microscopic components within single breast tumor sections and adaptation of established subtraction hybridization techniques to accept small input RNA sample and has been crucially dependent on the design of the tumor bank resource for histologically defined frozen breast tissues⁵⁻⁸.

Our specific hypothesis is that alteration of gene expression is responsible for the progression of DCIS to invasive breast cancer and the acquisition of the invasive phenotype. Our specific technical objectives are;

- 1.To identify and clone differentially expressed genes that may contribute to the invasive phenotype in-vivo. Novel microdissection and subtraction hybridization techniques will be used to directly compare gene expression between DCIS and adjacent early invasive ductal carcinoma cell populations within the same tumor specimen.
2. To study the role in breast cancer progression of altered expression of the candidate 'invasion genes' that have been identified in specific aim 1 by assessment of pattern of expression in-vivo and by manipulation of expression in breast cell lines.

BODY.**YEAR 1: SUMMARY.**

During year 1 of this project we had completed review of invasive ductal carcinomas in the Tumor Bank to identify cases that comprise in-situ and early invasive components, microdissectable within a single tissue block. We had proceeded to complete analysis of a second tumor case (tumor ^{dcis/inv} #2) and identified a number of differentially expressed cDNA's. We had also identified a technical problem with the magnetic bead subtraction assay that precluded further experiments with this assay. So we had begun to assess alternative molecular assays for analysis of differentially expressed mRNA and also begun to pursue the role in invasion of three of cDNA's - psoriasin, lumican and mammaglobin genes.

YEAR 2:

TECHNICAL OBJECTIVE 1. We have developed and performed RT-RDA ⁹ on small amounts of RNA extracted from MDA-MB-231 cells transfected with the psoriasin cDNA (see below) and compared parental cells with cells transfected with psoriasin, and found 36 apparently differentially cDNA's. To screen these for artifacts, cDNA's were blotted individually onto nitrocellulose membrane and re-probed with radiolabelled total cDNA from the initial representation step and we confirmed that 8/36 showed differential expression in the original sample. Although the assay produced a large number of 'false-positive' cDNA's (75%) we concluded that the RT-RDA assay⁹ was an acceptable assay as a first step to screen for differentially expressed genes in tumor samples.

We have then worked to adapt the assay to RNA obtained from microdissected tumors - smaller quantities and lesser quality RNA than from cultured cell lines. After 5 experiments on 4 microdissected tumors we have concluded that it is not practical to obtain sufficient quantities of RNA from subregions within typical tumor sections for the RT-RDA assay. So to confirm this conclusion and to progress with our aims we reviewed additional cases in the Tumor Bank

database for sections with pure DCIS or pure invasive ductal carcinoma and similar grade and cellularity. We then selected 2 sets of cases for analysis, each set comprising x3 DCIS cases to compare with x3 invasive ductal carcinoma cases. Frozen sections (20x20um) were then cut from each case, and sections pooled to create a DCIS pool and an invasive pool, prior to RNA extraction and RT-RDA. This RT-RDA experiment has yielded 13 cDNA's apparently overexpressed in the pre-invasive DCIS pool (see Appendix A). These include 6 known and 7 unknown genes and EST's. Amongst the former is the hevin-like protein that has previously been identified as down-regulated in metastatic in prostate cancer.

However, in parallel with the RT-RDA experiments above we have also investigated the possibility of applying microarray technology to our research question. We have done this because of the recent commercial availability of affordable membranes and analysis software, and the potential of this approach to compare/assess differential gene expression more efficiently than subtraction hybridization or RT-RDA. We view all three techniques as screening tools that can provide candidate cDNA's that need further confirmation and assessment by other tissue based techniques such as in-situ hybridization. We have carefully reviewed potential commercial array systems and discussed the issue of limited RNA samples with several companies. This has lead us to select the Research Genetics GeneFilters system ¹⁰.

We have subsequently obtained the Human GeneFilter GF200 filter and successfully shown that we can obtain adequate signals from labeled probes from 1 ug of microdissected total RNA for capture of images and analysis by the Pathways software. We are currently in the process of analyzing 3 new microdissected DCIS/invasive tumor samples. We are also now conducting exploratory experiments to validate the reproducibility of hybridization in our hands and the ability to be able to strip and reprobe each filter (claimed for 5 times) and are constructing cRNA internal standards. These standards (CNS specific genes already present on the GF200 filter) will be amplified by RT-PCR from human brain RNA and cloned into vectors suitable for producing

riboprobes to spike our RNA samples and provide additional internal controls for hybridization efficiency.

TECHNICAL OBJECTIVE 2. We have continued to pursue 2 potential 'invasion' genes, psoriasin, and lumican as outlined below. Since last years report we have successfully published a manuscript on a third gene, mammaglobin, (see Appendix D) but we are no longer pursuing this in the context of this project since our results suggest that mammaglobin is unrelated to invasion (but could be a useful clinical marker of axillary lymph node breast metastases)

Psoriasin (S100A7). We have previously identified psoriasin (S100A7) as differentially expressed between in-situ (DCIS) and invasive carcinoma. We have also shown that expression is relatively low in normal tissue and ductal hyperplasia, increased in atypical hyperplasia and highest in DCIS and frequently downregulated in invasive carcinoma ⁸.

- We have developed an anti-psoriasin polyclonal antibody and we have completed investigation of the role of persistent expression in invasive disease. Antibody specificity was confirmed by analysis of transfected cell lines and strong correlation between RT-PCR and in-situ hybridization detected levels of mRNA and western blot and immunohistochemistry detected protein, as well as its ability to detect the psoriasin protein in formalin fixed and paraffin embedded specimens. Persistence of psoriasin expression in invasive tumors was significantly associated with poor prognostic markers including ER and PR negative ($p < 0.0001$, $p = 0.0003$) and lymph node positive status ($p = 0.035$). Psoriasin protein expression is also associated with inflammatory infiltrates (all tumors excluding medullary where inflammation is a diagnostic criteria, $p = 0.0022$). These results suggest that psoriasin may be a marker of aggressive behaviour in invasive tumors and are also consistent with a function as a chemotactic factor (see Appendix E).

- We have examined the effect of psoriasin on invasive breast tumor cells. On the basis of our initial hypothesis in which we took the view that loss of psoriasin might facilitate invasiveness in the neoplastic breast cell, we transfected a CMV-psoriasin construct into a subline of MDA-MB-231 breast cells that do not express psoriasin and that are known to be invasive, tumorigenic and metastatic in an in-vivo metastasis model in our own hands and that have previously been shown to be amenable to genetic modulation of their metastatic properties. We isolated 2 MDA-231^{psoriasin} clones that demonstrate high and low mRNA and protein expression determined by Northern and Western Blot and have completed assessment of these cells by in-vitro growth and in-vitro Boyden chamber invasion assays. We have found that psoriasin overexpression has no significant effect on the growth or invasiveness of this already invasive breast tumor cell line. Therefore we have also decided to assess the effect of overexpression of psoriasin in a pre-invasive cell line and selected the MCF10AT model for these experiments. We have transfected CMV-psoriasin into MCF-10AT3B cells (using zeocin as a marker since they have previously been transfected with ras-neo) and after screening >25 zeocin resistant clones have obtained a single clone with overexpression detected by northern and western blot. We are now repeating transfection to obtain further clones prior to in-vitro assessment of growth and invasiveness and in-vivo study of the effect of psoriasin on early tumorigenesis and progression (see Appendix B).
- We have also pursued the cell biology of psoriasin in breast. In-situ hybridization consistently shows that psoriasin mRNA expression is restricted to epithelial cells in skin and breast tumors. Psoriasin protein, studied by immunohistochemistry is also localized predominantly but not exclusively to epithelial cells, but with both cytoplasmic and nuclear staining (the latter most prominent in breast tumor cells). Therefore to pursue the possible intracellular interactions of psoriasin we have searched for interacting proteins in a normal breast cell library using the yeast 2-hybrid assay. From the first screen we have identified 4 positive clones. The first two genes are both recently identified components of the centrosome, RanBPM and spindle pole body protein hGCP3¹¹, while the other two cDNAs are a transcription factor binding protein and a gene of

unknown function (CXX-1). The co-incidental finding of 2 centrosome related proteins encourages us to pursue in the future the role of the interaction between psoriasin, RanBPM and hGCP3¹¹ in early progression towards the invasive phenotype (see Appendix C).

Lumican. We previously identified lumican mRNA as differentially expressed between the stroma adjacent to pre-invasive and central invasive components of early breast tumors. RT-PCR and in situ hybridization study confirmed the presence of lumican mRNA in fibroblast-like cells within stroma of most tumors, with highest levels adjacent to in-situ components and beyond the invasive edge. Higher expression in the invasive tumor was also associated with poor prognostic markers¹²

- Further study of lumican and other members of the small leucine-rich proteoglycan (SLRP) gene family in breast tissues has been completed (in collaboration with Dr Peter Roughley, Montreal) to explore their role in breast tumor progression. Lumican and decorin are expressed by similar fibroblast-like cells and are relatively abundant, while biglycan and fibromodulin are only detected occasionally and at low levels in breast tissues. However, while lumican mRNA expression was significantly increased in tumors (n=34, p<0.0001), decorin mRNA was decreased (p=0.0002) in neoplastic relative to adjacent normal stroma. This was accompanied by similar changes in both lumican (p=0.0122) and decorin (similar trend but p=ns) proteins. Alteration of lumican expression in breast tumor stroma may also be manifested by discordance between mRNA and protein localization in some tumors, where some areas (mostly central regions) can demonstrate mRNA expression by in-situ hybridization but no detectable protein in parallel sections assessed both by immunohistochemistry and microdissection + western blot (see Appendix F)¹³.

We are currently studying the issue of reciprocal regulation of lumican and decorin in cultured cell lines. We have screened a panel of breast and fibroblast cell lines by RT-PCR and western blot and shown that lumican and decorin expression is restricted to fibroblasts. We are now performing co-culture assays to understand the role and effect of the status of the epithelial cells in influencing

lumican and decorin expression in adjacent fibroblasts. We have also attempted to transfect human lumican and decorin cDNA's into an immortalized murine mammary fibroblast line to study the effect of this on fibroblast function and neoplastic syngeneic carcinoma cells utilizing both in-vitro 3-D co-culture, and in-vivo study of mixed fibroblast and tumor populations (in collaboration with Dr C Roskelley, UBC). However we have been unsuccessful as yet in obtaining successful transfectants. Given the known inhibitory effect of decorin on cell growth we are now considering the alternative strategy of re-cloning the lumican and decorin cDNA's into an inducible tet expression system.

KEY RESEARCH ACCOMPLISHMENTS

- We have completed microdissection and partial analysis by Subtraction Hybridization techniques and membrane filter cDNA array hybridization of matched DCIS and invasive components for 5 breast tumor cases.
- We have identified and pursued 3 potential 'invasion' genes, psoriasin (S100A7), lumican and mammaglobin, that had not been previously explored in breast cancer progression
- We have shown that persistent S100A7 expression correlates with poor prognostic features in invasive breast tumors and are currently exploring the effect of modulation of S100A7 in cell lines
- We have shown that expression of lumican and decorin stromal matrix proteins is altered and that these are the most abundant members of the small leucine-rich proteoglycans in breast tissues and that altered regulation of these two genes occurs in tumors and is distinct. Given that the small leucine-rich proteoglycans are important in collagen fibrillogenesis we are now pursuing their role in tumor invasion and progression.
- We have shown that while mammaglobin expression may not relate to invasion, expression of the gene may be a valuable marker for detection of breast cancer cells metastatic to lymph nodes

REPORTABLE OUTCOMES

Papers
Leygue E, Snell L, Dotzlaw H, Hole K, Hiller T, Roughley P, Watson P, Murphy L, "Expression of Lumican in human breast carcinoma" Cancer Research 58(7): 1348-1352, 1998.
Leygue E, Snell L, Dotzlaw H, Hole K, Hiller T, Roughley P, Watson P, Murphy L, "Mammaglobin, a potential marker of breast micrometastasis" In press J Path 1999 *
A-Haddad S, Zhang Z, Leygue E, Snell L, Huang A, Niu Y, Hiller T, Hone K, Murphy LC, Watson PH. The role of psoriasin (S100A7) in invasive breast cancer. In press, Am J Pathology. 1999 *
Leygue E, Snell L, Dotzlaw H, Hole K, Hiller-Hitchcock T, Murphy LC, Roughley PJ, Watson P,. "Lumican and decorin are differentially expressed in human breast carcinoma" submitted to J Path, Aug 1999 *
Chapters
Watson PH, Hiller T, Snell LS, Murphy LC, Leygue E, Dotzlaw H, Kossakowska A, Kulakowski A. "Update to : microdissection RT-PCR analysis of gene expression in pathologically defined frozen tissue sections" in "the PCR technique: RT-PCR, editor Paul Siebert, Eaton Publishing. 1997
Watson PH, Leygue E, Murphy LC. "Molecules in focus- psoriasin (S100A7)" Int J Biochem Cell Biol. 30(5): 567-571. 1998
Abstracts
Leygue E, Snell L, Dotzlaw, Hole, Hiller T, Watson P, Murphy L. "Differential expression of mammaglobin mRNA during breast tumorigenesis". 20th Breast Cancer Symposium, San Antonio, Texas, Dec 1997
Leygue E, Snell L, Dotzlaw H, Hole K, Hiller-Hitchcock T, Murphy LC, Roughley PJ, Watson P,. "Lumican and decorin are differentially expressed in human breast carcinoma" submitted 21st Breast Cancer Symposium, San Antonio, Texas, Dec 1998 *
A-Haddad S, Zhang Z, Leygue E, Snell L, Huang A, Niu Y, Hiller T, Hone K, Murphy LC, Watson PH. The role of psoriasin (S100A7) in invasive breast cancer. AACR Philadelphia, April 1999 *

* = new outcome or revised outcome specific to Year 2 of the project

CONCLUSIONS

Elucidation of the molecular changes involved in the development of the invasive phenotype is a critical clinical question because the lethal effects of distant metastasis can only occur after the onset of invasive capability and the ability to assess these genetic alterations may offer markers of risk of invasive disease in pre-invasive lesions.

We have identified, microdissected and assessed differential gene expression in 5 tumors by subtraction hybridization, RT-RDA, and microarray techniques. Our progress with Objective 1 has been slowed by technical issues relating to the first 2 techniques, however we now anticipate that we will be able to complete the Objective 1 by end of this grant year. Our progress with Objective 2 has been steady. We have pursued the roles of 3 potential invasion genes, mammaglobin, psoriasin, and lumican and continue to work on the latter 2 genes which show potential as important factors in the process of invasion.

In the coming year we will complete microdissection and analysis of 12 cases, screen a subset of further candidate genes to confirm differential expression, and continue to pursue the cell biology of psoriasin and lumican as it relates to the process of invasion.

REFERENCES

1. A) Norton L, Rosen PP, Rosen N. Refining the origins of breast cancer. Editorial *Nature Medicine*, 1: 1250-51 B) N.I.H. Consensus Development Conference Statement: early stage breast cancer: June 18-21,1990. C) Ernster VL, Barclay J, Kerlikowske K, Grady D, Henderson IC. Incidence of and treatment for ductal carcinoma in-situ of the breast. *JAMA* 275: 913-918,1996
2. A) Silverstein ML Lagios MD Craig PH, Waisman JR Lewinsky BS Colburn WJ Poller DN A prognostic index for ductal carcinoma in situ of the breast. *Cancer* 77: 2267-74 1996. B) Schnitt SJ, Harris JR, Smith BL Developing a prognostic index for ductal carcinoma in situ of the breast. Are we there yet? Editorial, *Cancer* 77: 2189-92, 1996, C) Morrow M. The natural history of ductal carcinoma in-situ , Implications for clinical decision making. Editorial *Cancer* 76: 1113-1115, 1995. D) Kerlikowske K, Barclay J, Grady D, Sickles EA, Ernster V J Comparison of risk factors for ductal carcinoma in situ and invasive breast cancer. *Natl Cancer Inst* Jan 1;89(1):76-82 1997; E) Allred DC, O'Connell P, Fuqua SAW. Biomarkers in early breast neoplasia. *J Cell Biochem* 17G: 125,1993
3. Liotta, L.A., Tumor invasion and metastasis: role of the basement membrane. *Am.J. Path.*, 117:339-348,1984; Dickson, R.B. and Lippman, M.E., Molecular determinants of growth, angiogenesis and metastasis in breast cancer. *Semin. Oncol.*, 19:286-298,1992
4. A) O'Connell P, Pekkel V, Fuqua SA, Osborne CK, Clark GM, Allred DC Analysis of loss of heterozygosity in 399 premalignant breast lesions at 15 genetic loci. *J Natl Cancer Inst* 1998 May 6;90(9):697-703; B) Radford DM, Fair KL, Phillips NJ, Ritter JH, Steinbrueck T, Holt MS, Donis-Keller H. Allelotyping of ductal carcinoma in situ of the breast: deletion of loci on 8p, 13q, 16q, 17p and 17q. *Cancer Res* 1995 Aug 1;55(15):3399-3405
5. Hiller, T., L. Snell, Watson P. "Microdissection RT-PCR analysis of gene expression in pathologically defined frozen tissue sections." *Biotechniques* 21(1): 38-44, 1996.
6. Leygue, E. R., Watson,PH, Murphy LC. "Identification of differentially expressed genes using

minute amounts of RNA.” *Biotechniques* 21(6): 1008-12,1996.

7. Watson P, Snell L, Parisien M. “The Role of a Tumor Bank in Translational Research”
Canadian Medical Association Journal, 155, 281-283, 1996
8. Leygue E., Hiller T., Snell L., Hole K., Dotzlaw H., Murphy L., Watson P. Differential expression of Psoriasin (S100A7) mRNA between in-situ and invasive human breast cancer.
Cancer Res. 56, 4606-4609. 1996
9. Hubank M, Schatz DG. Identifying differences in mRNA expression by representational difference analysis of cDNA. *Nucleic Acids Res* 1994 Dec 25;22(25):5640-5648
10. Research Genetics . <http://www.resgen.com/>.
11. A) Nakamura M, Masuda H, Horii J, Kuma K, Yokoyama N, Ohba T, Nishitani H, Miyata T, Tanaka M, Nishimoto T. When overexpressed, a novel centrosomal protein, RanBPM, causes ectopic microtubule nucleation similar to gamma-tubulin. *J Cell Biol* 143:1041-1052, 1998; B) Murphy SM, Urbani L, Stearns T. The mammalian gamma-tubulin complex contains homologues of the yeast spindle pole body components spc97p and spc98p. *J Cell Biol* 141:663-674, 1998;
12. Leygue E, Snell L, Dotzlaw H, Hole K, Hiller T, Roughley P, Watson P, Murphy L, “Expression of Lumican in human breast carcinoma” *Cancer Research* 58(7): 1348-1352, 1998.
13. Leygue E, Snell L, Dotzlaw H, Hole K, Hiller-Hitchcock T, Murphy LC, Roughley PJ, Watson P., “Lumican and decorin are differentially expressed in human breast carcinoma” submitted to *J Path*, Aug 1999

APPENDICES

- Appendix A) Tumor case analysis figures and data – RT-RDA and microarray.
- Appendix B) Psoriasin transfected cell lines – analysis
- Appendix C) Psoriasin interacting proteins - Yeast –2 Hybrid analysis
- Appendix D) Leygue E, Snell L, Dotzlaw H, Hole K, Hiller T, Roughley P, Watson P, Murphy L, “Mammaglobin, a potential marker of breast micrometastasis” In press J Path 1999
- Appendix E) Al-Haddad S, Zhang Z, Leygue E, Snell L, Huang A, Niu Y, Hiller T, Hole K, Murphy LC, Watson PH. The role of psoriasin (S100A7) in invasive breast cancer. In press, Am J Pathology. 1999
- Appendix F) Leygue E, Snell L, Dotzlaw H, Hole K, Hiller-Hitchcock T, Murphy LC, Roughley PJ, Watson P,. “Lumican and decorin are differentially expressed in human breast carcinoma” submitted to J Path, Aug 1999

APPENDIX A

Figures for Differential Gene Expression Experiments Involving Both RDA and Filter Arrays

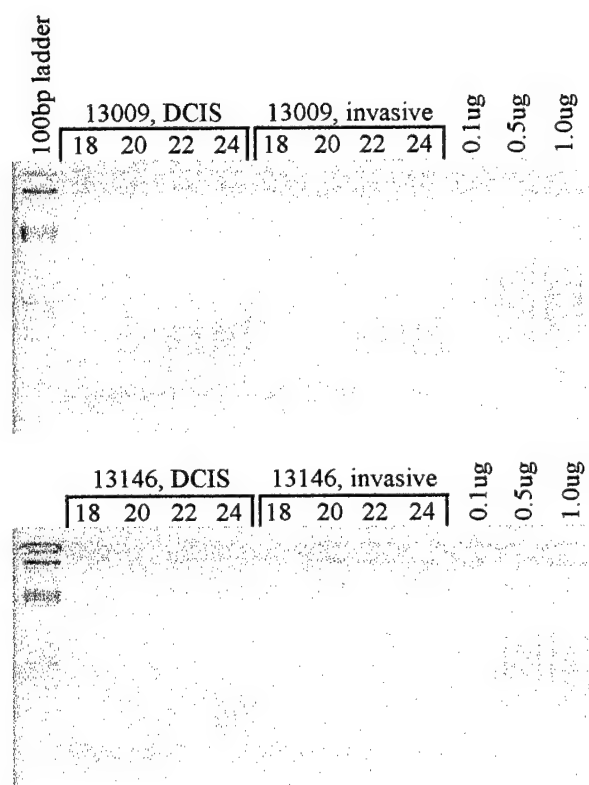


Figure 1: Optimization of RDA pilot reactions from microdissected tumors.

Samples were removed at 18, 20, 22 and 24 PCR cycles and run on a 1.5% agarose gel with controls. The samples were compared to the controls - a known amount of Sau3AI digested genomic spleen DNA looking for an optimum amount of 0.5ug per sample. Tumor numbers are as listed.

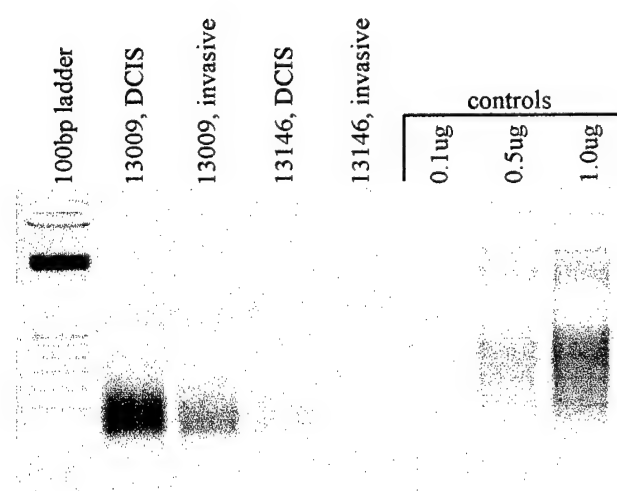


Figure 2: Scaled up RDA reactions from figure 1. For tumor 13009, the PCR hot bonnet lid failed, thus resulting in the loss of this experiment. ie. in lane 1 (13009, DCIS) the sample is much more prominent, probably resulting in a misrepresentation of the cDNAs in this tumor. For tumor 13146, the invasive sample repeatedly failed to amplify, thus resulting in the loss of this experiment. It has been determined that the quantity and quality of RNA obtained from microdissected tumors does not make RDA a good candidate technique for further studies involving microdissection.

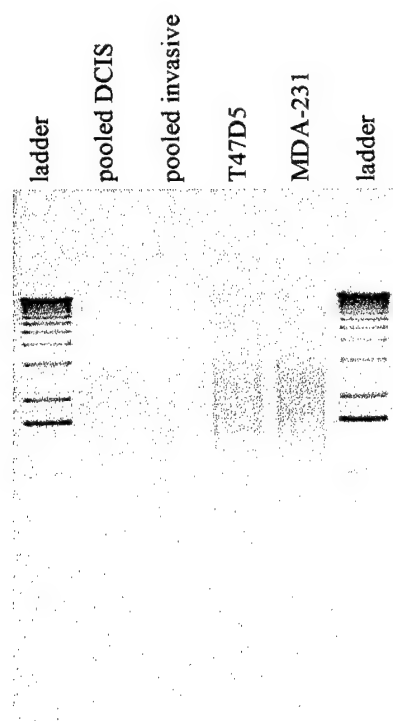


Figure 3: Tumor and cell line cDNA. Pooled DCIS and pooled invasive samples represent 4 tumor cases whose RNA has been combined to try to increase the quantity. T47D5 and MDA-231 are representative cell line controls. Equal OD amounts were loaded (2ug), yet are not comparable. Potentially, the tumor samples are degraded due to the collection procedure and therefore the quality and quantity is not the same as that which is obtained from cell lines.

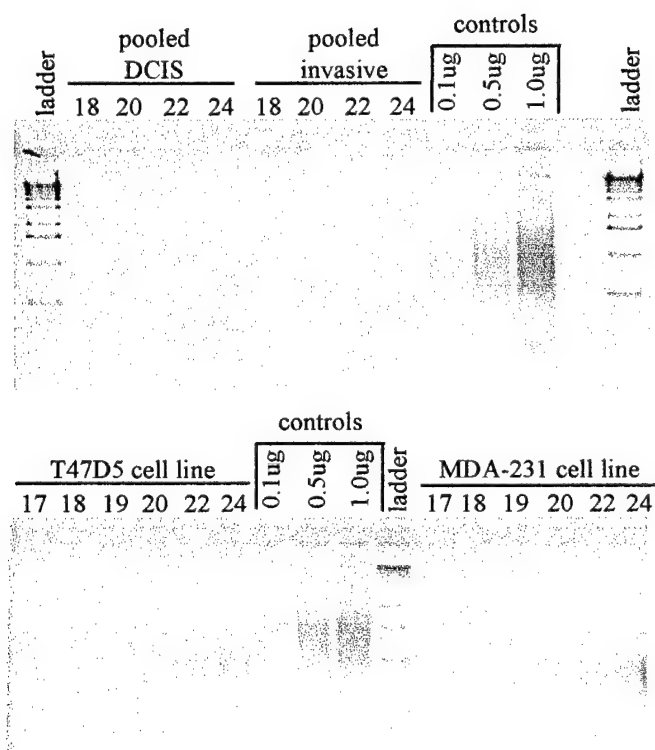


Figure 4: RDA pilot reactions comparing pooled tumor samples and cell lines. Samples were removed at a specific PCR cycle number and run on a 1.5% agarose gel with Sau3AI digested genomic spleen DNA controls. Note that the cell lines amplify much better than the tumor samples.

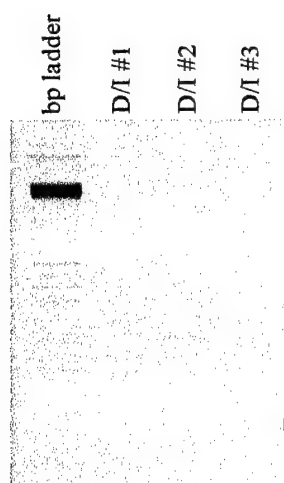


Figure 5: Isolated RDA bands. Three bands were isolated from DCIS vs invasive pooled RDA samples (D/I #1, D/I #2, D/I #3). All bands are representative of genes which are potentially overexpressed in DCIS but not in invasive tumors. Each band may contain more than one gene.

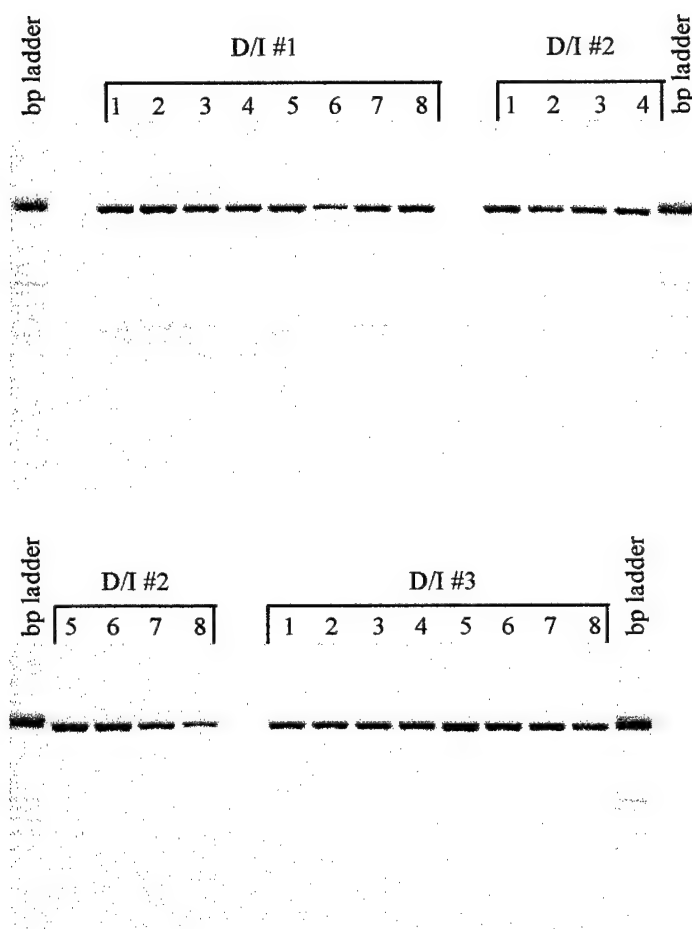


Figure 6: cDNA RDA clones. All lanes represent single clones from the isolated RDA bands. Refer to the subtable of RDA clones where, for example, p#1-2 = D/I #1 lane 2. Overall, 15 of the 24 clones were sequenced, giving 6 known genes, 5 EST's and 2 unknowns.

A**B**

Figure 7:Hybridized filter arrays. (A) A Research Genetics filter array (#GF200), hybridized with a microdissected DCIS tumor sample. **(B)** The same array hybridized with a probe made from microdissected invasive tumor. Both samples originated from the same case, tumor# 13146. Note the similar hybridization patterns.

TUMOR CASES SELECTED AND/OR USED
FOR RT-RDA AND MICROARRAY FILTER EXPERIMENTS:

USAMRMC Project: Year 2.

Tumor Number	MDX method	Technique	Result
B13009A,B	Mdx	RDA	PCR machine hot-bonnet problem
B13146B	Mdx	RDA	wouldn't amplify
13146B	Mdx	RDA	wouldn't amplify
11612B	Mdx	RDA	wouldn't amplify
10603A	Mdx	RDA	wouldn't amplify
Pooled Set1: DCIS=9857B,10631 B10078A,9055C inv=8666A,7992A, 9110A, 10571B	FS	RDA	worked => 3 bands, 10 different clones –see subtable below
Pooled Set2: DCIS=10953B, 12166A,12438B inv=8196A,7952A, 7949B	FS	For RDA	Not sectioned yet
10654	Mdx	GeneFilter #201	completed, to be analyzed
13009	Mdx	GeneFilter	not enough DCIS RNA
10603	Mdx	GeneFilter #200	Completed, to be analyzed
13146	Mdx	GeneFilter #200	Completed, under analysis, refer to GeneFilter Comparison report

Mdx = frozen sections cut and subregions microdissected from within each section

FS = frozen sections cut and used without further microdissection

Subtable of RDA clones from pooled Set1

Clone #	Gene
p#1-2	matrix Gla protein
p#1-4	DVS27 related protein
p#1-5	unknown
p#1-6	EST
p#1-7	unknown
p#2-1	Ca ⁺⁺ transporting ATPase (ATP2B1)
p#2-2	EST
p#2-6	EST
p#2-7	hevin like protein, hevin
p#2-8	EST
p#3-1, p#3-4	EST
p#3-2, p#3-5	RNA helicase p68
p#3-6	tyrosine aminotransferase

GeneFilter Comparison Report

GeneFilter1 Name:

13146 DCIS 20 HOUR E

Researcher/Laboratory:

Kate Hole

Date:

9/21/99

GeneFilter2 Name:

13146 INVASIVE 20 HO

Researcher/Laboratory:

Kate Hole

Date:

9/21/99

Description:

microdissected tumor #13146 DCIS, 20 hour exposure

Cell Width = 7

Background Average = 98.117

Maximum Image Intensity = 65535

Minimum Image Intensity = 20

Description:

microdissected tumor # 13146 invasive 20 hour exposure, some saturated spots

Cell Width = 5

Background Average = 65.263

Maximum Image Intensity = 65535

Minimum Image Intensity = 14

GeneFilter 1: 13146 DCIS 20 HOUR E

GeneFilter 2: 13146 INVASIVE 20 HO

F-G-R-C	CDNA ID	INTENSITIES			CLUSTER ID	NID	CYTO	STS	
		GF1	GF2	RATIO	DIFF			NAME	ACC
1-C-29-11	841641	1491	582	2.56	908.83	g2217864	11q13	WI-16756	G213.
Bld: Unigene-18	Chrom: 11	Gene: CCND1						Cyclin D1 (PRAD1; parathyroid adenomatosis 1)	
1-F-17-8	840940	4570	1785	2.56	2785.53	g2216790		SHGC-30876	G273.
Bld: Unigene-18	Chrom:	Gene: PABP1						Poly(A)-binding protein-like 1	
1-G-3-5	160838	4065	1624	2.50	2440.55	g893587			
Bld: Unigene-19	Chrom:	Gene:						"Human SWI/SNF complex 170 KDa subunit (BAF170) mRNA, complete cds"	
1-H-2-4	810612	5029	1813	2.77	3215.84	g2189615			
Bld: Unigene-19	Chrom: 7	Gene:						"Human mRNA for calgizzarin, complete cds"	
1-H-13-8	773254	2400	952	2.52	1447.56	g2106496		WI-7518	G065.
Bld: Unigene-18	Chrom: 1	Gene:						PTB-ASSOCIATED SPLICING FACTOR	
2-A-15-6	123065	1795	604	2.97	1190.43	g748266			
Bld: Unigene-19	Chrom:	Gene:							ESTs

Human GeneFilter, Release 1 (GF200)

Research Genetics, Inc.

Pathways

GeneFilter 1: 13146 DCIS 20 HOUR E

GeneFilter 2: 13146 INVASIVE 20 HO

F-G-R-C	CDNA ID	INTENSITIES				CLUSTER ID	NID	CYTO	STS	
		GF1	GF2	RATIO	DIFF				NAME	ACC
2-A-13-8	140759	1878	726	2.59	1152.15	Hs.28715	g838928			
Bld: Unigene-19 Chrom:										
2-A-3-11	296773	868	310	2.80	557.50	Hs.50429	g1231358			ESTs
Bld: Unigene-19 Chrom:										
2-D-30-11	239711	4928	1643	3.00	3284.38	Hs.93372	g1057739			ESTs
Bld: Unigene-19 Chrom:										
2-G-26-9	233179	549	217	2.53	332.04	Hs.39749	g1055484			ESTs
Bld: Unigene-19 Chrom:										
2-G-4-10	296749	2088	697	3.00	1390.85	Hs.39945	g1231344			ESTs
Bld: Unigene-19 Chrom:										
2-G-2-12	140635	1919	723	2.66	1196.49	Hs.95893	g839583		WI-13707	G233
Bld: Unigene-19 Chrom: 9										

Normalization Method:

The average intensity of all control positives are calculated for probe A and probe B. A factor is calculated to bring each filter up to equal intensity ranges.

GeneFilter Comparison Report

GeneFilter1 Name:

13146 DCIS 20 HOUR E

Researcher/Laboratory:

Kate Hole

Date:

9/21/99

GeneFilter2 Name:

13146 INVASIVE 20 HO

Researcher/Laboratory:

Kate Hole

Date:

9/21/99

Description:

microdissected tumor #13146 DCIS, 20 hour exposure

Cell Width = 7

Background Average = 98.117

Maximum Image Intensity = 65535

Minimum Image Intensity = 20

Description:

microdissected tumor # 13146 invasive 20 hour exposure, some saturated spots

Cell Width = 5

Background Average = 65.263

Maximum Image Intensity = 65535

Minimum Image Intensity = 14

GeneFilter 1: 13146 DCIS 20 HOUR E

GeneFilter 2: 13146 INVASIVE 20 HO

F-G-R-C	cDNA ID	INTENSITIES			CLUSTER ID	NID	CYTO	STS	
		GF1	GF2	RATIO	DIFF			NAME	ACC
1-A-28-10	898317	313	1311	-4.19	-997.48	Hs.77007		WI-16281	G246.
Bld: Unigene-18	Chrom: 13	Gene:						"Human Hs-cul-4A mRNA, partial cds"	
1-E-6-6	245136	389	1647	-4.23	-1257.19	Hs.16349		WI-6254	G060.
Bld: Unigene-19	Chrom: 16	Gene:						"Homo sapiens KIAA0432 mRNA, complete cds"	
1-G-19-7	128243	1130	5691	-5.03	-4560.82	Hs.94382	10q11-q24	WI-11741	G215.
Bld: Unigene-19	Chrom: 10	Gene: ADK						Adenosine kinase	
1-G-20-8	825295	1248	6979	-5.59	-5731.23	Hs.70008		SHGC-15376	G150.
Bld: Unigene-18	Chrom: 16	Gene:						LOW-DENSITY LIPOPROTEIN RECEPTOR PRECURSOR	
1-H-14-4	70002	718	3259	-4.54	-2541.20	Hs.23978		SHGC-11345	G145.
Bld: Unigene-19	Chrom: 19	Gene:						"Human mRNA for KIAA0138 gene, complete cds"	
1-H-29-5	171936	563	3059	-5.44	-2496.50	Hs.89692		SHGC-31541	G293.
Bld: Unigene-19	Chrom:	Gene: HPCA						Hippocalcin	

Human GeneFilter, Release 1 (GF200)

Research Genetics, Inc.

Pathways

GeneFilter 1: 13146 DCIS 20 HOUR E

GeneFilter 2: 13146 INVASIVE 20 HO

F-G-R-C	CDNA ID	INTENSITIES			CLUSTER ID	NID	CYTO	STS	
		GF1	GF2	RATIO				NAME	ACC
1-H-4-6	150623	272	1591	-5.85	Hs.79228	g865091	9q21.32-q21.33	WI-9204	G071
Bld: Unigene-19	Chrom: 11	Gene: HNRPK			Heterogeneous nuclear ribonucleoprotein K				
1-H-4-7	275738	2806	13446	-4.79	Hs.23118	g967342	8q22	SHGC-31642	G285
Bld: Unigene-19	Chrom: 8	Gene: CA1			Carbonic anhydrase I				
1-H-5-9	700302	1834	8714	-4.75	Hs.95821	g1927905			
Bld: Unigene-18	Chrom:	Gene:			"Human osteoclast stimulating factor mRNA, complete cds"				
1-H-9-10	950578	1667	7760	-4.65	Hs.83916				
Bld: Unigene-18	Chrom:	Gene:			"Human NADH:ubiquinone oxidoreductase subunit B13 (B13) mRNA, complete cds"				
1-H-10-10	46054	353	1516	-4.29	Hs.79371	g873755		CHLC.UTR 05505 U09002	G107
Bld: Unigene-18	Chrom: 16	Gene:			an N-methyl-D-aspartate receptor modulatory subunit 2A (hNR2A) mRNA, complete cds"				
1-H-12-10	897806	842	3502	-4.16	Hs.82765			SHGC-35483	G298
Bld: Unigene-18	Chrom: 14	Gene:			"Human MOP1 mRNA, complete cds"				
1-H-5-11	810942	2118	9327	-4.40	Hs.75253	g2184287			
Bld: Unigene-18	Chrom: X	Gene:			sapiens mRNA for NAD (H)-specific isocitrate dehydrogenase gamma subunit precursor				
1-H-10-11	77533	1851	13143	-7.10	Hs.63458	g660610			
Bld: Unigene-18	Chrom: 10	Gene:			H.sapiens mRNA for InSP3 5-phosphatase				
1-H-28-11	843049	1296	10487	-8.09	Hs.89699	g2216199		SHGC-35380	G285
Bld: Unigene-18	Chrom:	Gene:			CDC21 HOMOLOG				
1-H-3-12	490368	5093	20504	-4.03	Hs.75626	g1697567	1p13	SHGC-10823	G111
Bld: Unigene-18	Chrom: 1	Gene: CD58			"CD58 antigen, (lymphocyte function-associated antigen 3)"				
1-H-7-12	788185	1768	7562	-4.28	Hs.51233	g2167079		WI-15306	G242
Bld: Unigene-19	Chrom: 8	Gene:			"Homo sapiens TRAIL receptor 2 mRNA, complete cds"				
1-H-28-12	843426	1688	10220	-6.05	Hs.103102	g2219100			
Bld: Unigene-19	Chrom:	Gene:			"ESTs, Weakly similar to WWP2 [H.sapiens]"				
2-A-26-9	292357	738	3056	-4.14	Hs.38036	g1243690			
Bld: Unigene-19	Chrom:	Gene:			EST				

GeneFilter 1: 13146 DCIS 20 HOUR E

GeneFilter 2: 13146 INVASIVE 20 HO

F-G-R-C	CDNA ID	INTENSITIES				CLUSTER ID	NID	CYTO	STS	
		GF1	GF2	RATIO	DIFF				NAME	ACC
2-A-26-10	245219	526	2237	-4.26	-1711.55	Hs.47832	g1239178		SHGC-44455	G314: ESTs
Bld: Unigene-19	Chrom:	Gene:								
2-C-5-7	296177	244	1061	-4.35	-817.17	Hs.22338	g1226595		SHGC-19242	G311: ESTs
Bld: Unigene-19	Chrom:	Gene:								
2-D-27-3	283398	529	2385	-4.51	-1856.48	Hs.8769	g1201484			
Bld: Unigene-19	Chrom:	Gene:					"ESTs, Highly similar to HEMOGLOBIN ZETA CHAIN [Homo sapiens]"			
2-E-12-2	66894	1093	4521	-4.13	-3427.19	Hs.13094	g680621		WI-14740	G215: ESTs
Bld: Unigene-19	Chrom: 3	Gene:					"ESTs, Weakly similar to HYPOTHETICAL 38.8 KD PROTEIN IN MIC1-SRBS INTERGENIC REGION [S.cerevisiae]"			
2-G-1-3	295630	1229	5162	-4.20	-3933.28	Hs.47501	g1218977		SHGC-37435	G305: ESTs
Bld: Unigene-19	Chrom:	Gene:					"ESTs, Highly similar to hOrc2p [H.sapiens]"			
2-G-12-4	203931	116	471	-4.06	-354.64	Hs.6006	g1005314		SHGC-36295	G301: ESTs
Bld: Unigene-19	Chrom:	Gene:								
2-G-21-4	293078	526	2419	-4.60	-1893.02	Hs.11648	g1224880		WI-16393	G219: ESTs
Bld: Unigene-19	Chrom: 3	Gene:								
2-G-30-4	123604	504	2633	-5.22	-2128.84	Hs.12003	g750577		WI-11871	G212: ESTs
Bld: Unigene-19	Chrom: 9	Gene:								
2-G-21-5	129563	780	3527	-4.52	-2746.82	Hs.15885	g764133		WI-16757	G238: ESTs
Bld: Unigene-19	Chrom: 1	Gene:								
2-G-16-7	136064	416	1679	-4.04	-1263.27	Hs.24759	g790129			
Bld: Unigene-19	Chrom:	Gene:								
2-H-24-3	229467	1451	5858	-4.04	-4407.06	Hs.39943	g1057596			
Bld: Unigene-19	Chrom: 19	Gene:					"ESTs, Highly similar to MKR2 PROTEIN [Mus musculus]"			
2-H-6-7	131563	562	3179	-5.66	-2617.87	Hs.23630	g779111			
Bld: Unigene-19	Chrom:	Gene:								
2-H-8-9	201317	636	2639	-4.15	-2002.38	Hs.36148	g986291			
Bld: Unigene-19	Chrom:	Gene:								

GeneFilter 1:	13146 DCIS 20 HOUR E
GeneFilter 2:	13146 INVASIVE 20 HO

F-C-R-C	cDNA ID	INTENSITIES				CLUSTER ID	NID	CYTO	STS	
		GF1	GF2	RATIO	DIFF				NAME	ACC
2-H-21-10	295106	699	3276	-4.68	-2576.69	Hs.50058	g1273644		SHGC-44501	G315:
Bld: Unigene-19 Chrom:		Gene:				ESTs				
2-H-26-11	136984	529	2313	-4.37	-1784.59	Hs.97277	g792750		WI-17313	G219:
Bld: Unigene-19 Chrom: 3		Gene:				ESTs				

Normalization Method:

The average intensity of all control positives are calculated for probe A and probe B. A factor is calculated to bring each filter up to equal intensity ranges.

APPENDIX B

CELL LINE	DOUBLING TIME (DAYS) $\bar{x} \pm \text{SEM (n)}$	INVASION (%) $\bar{x} \pm \text{SEM (n)}$
MDAMB231 (parent)	$1.03 \pm 0.05 (4)$	$23.4 \pm 6.8 (3)$
Vector alone (CL6VA1)	$1.32 \pm 0.13 (4)$	$22.9 \pm 3.3 (3)$
Vector alone (CL71A1)	$1.26 \pm 0.04 (4)$	$32.9 \pm 5.7 (3)$
Psoriasin + (CL6FA1)	$1.04 \pm 0.02 (4)$	$34.5 \pm 6.0 (3)$
Psoriasin + (CL7FB2)	$1.27 \pm 0.06 (4)$	$30.8 \pm 1.9 (3)$
Psoriasin + (CL7FD3)	$1.13 \pm 0.07 (3)$	$21.4 \pm 4.7 (3)$

There are no statistically significant differences between the psoriasin expressing clones and the non-expressing controls in terms of doubling time or % invasion.

APPENDIX C

Psoriasin interacting proteins

Yeast 2-hybrid assay data

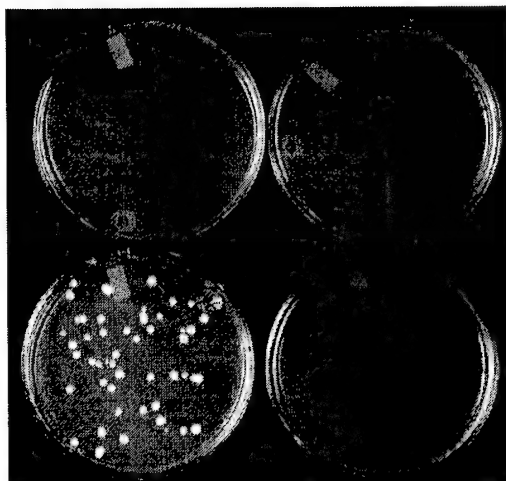


Fig 1: Test for an interaction with the bait plasmid containing no bait cDNA, using isolated plasmid containing RanBPM with Gal4 AD (clone 6-3) co-transformed with bait Gal4 BD plasmid (pGBT9). Bottom left plate contains media deficient in tryptophan and leucine. Growth confirms the presence of both plasmids. Remaining three plates are all deficient in tryptophan, leucine and histidine. No growth confirms no activation of histidine gene after 14 days incubation. In order to activate histidine gene, a bait protein is required for AD and BD to interact which activates the histidine gene and allows growth.

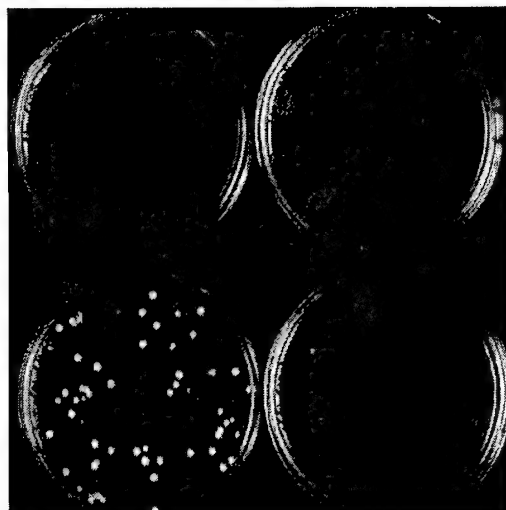


Fig 2: Test for interaction with an unrelated bait protein (Rad 18) using isolated plasmid containing RanBPM with Gal4 AD (clone 6-3) co-transformed with Rad18 cloned after Gal4 BD. In this case the bait protein is Rad18, which is a DNA repair gene found in yeast. Growth on bottom left plate deficient in tryptophan and leucine confirms presence of both plasmids. Remaining three plates are all deficient in tryptophan, leucine and histidine. No growth confirms no histidine activation after 14 days incubation. In order to activate histidine gene, the bait and RanBPM interaction must be specific in order for the Gal4 AD and BD to interact which activates the histidine gene and allows growth.

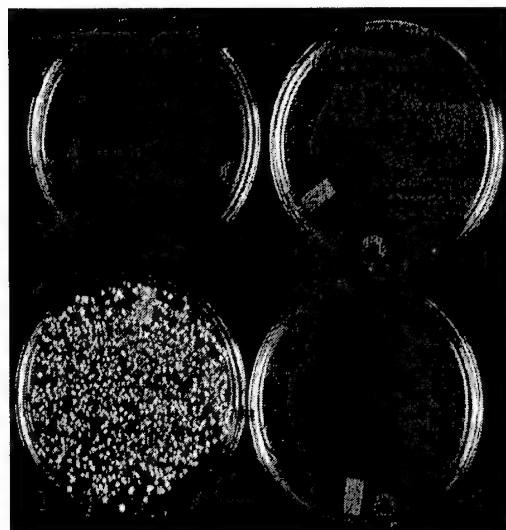


Fig 3: Test for autoactivation of histidine selection gene by isolated RanBPM plasmid. Yeast transformed with RanBPM plasmid (6-3) only. Lower left shows yeast plated on media deficient in leucine and growth proves presence of RanBPM plasmid. Top left plate deficient in tryptophan, no bait plasmid present to allow growth. Top right deficient in tryptophan and leucine, absence of growth confirms need for both psoriasin and RanBPM plasmids. Lower right plate deficient for histidine, absence of growth confirms need for the psoriasin-RanBPM interaction of fusion proteins containing BD and AD respectively, to get activation of histidine gene under control of Gal4 promoter. Clone 6-3 does not autoactivate the histidine gene. All plates incubated for 14 days.

APPENDIX D

MAMMAGLOBIN, A POTENTIAL MARKER OF BREAST CANCER NODAL METASTASIS

ETIENNE LEYGUE¹*, LINDA SNELL², HELMUT DOTZLAW¹, KATE HOLE², SANDY TROUP², TAMARA HILLER-HITCHCOCK²,
LEIGH C. MURPHY¹ AND PETER H. WATSON²

¹Department of Biochemistry and Molecular Biology, University of Manitoba, Faculty of Medicine, Winnipeg,
Manitoba R3E 0W3, Canada

²Department of Pathology, University of Manitoba, Faculty of Medicine, Winnipeg, Manitoba R3E 0W3, Canada

SUMMARY

The *Mammaglobin* gene, a breast-specific member of the uteroglobin gene family, has been previously identified as being overexpressed in some breast tumours, but the cellular origin and relationship to tumour progression are unknown. Using a subtractive hybridization approach, *mammaglobin* mRNA has also been found to be overexpressed in the *in situ* compared to the invasive element within an individual breast tumour. Further study by *in situ* hybridization performed in 13 breast tumours, selected to include normal, *in situ*, and invasive primary tumour elements, and in most cases axillary lymph node metastases, revealed that *mammaglobin* expression occurs in all elements, is restricted to epithelial cells, and is significantly increased in tumour cells compared with normal cells ($p < 0.04$). Analysis of *mammaglobin* expression within 20 independent primary breast tumours and their corresponding axillary lymph nodes revealed that all 13 lymph nodes positive and none of the seven nodes negative for metastatic breast carcinoma by histology were *mammaglobin*-positive by reverse transcription-polymerase chain reaction (RT-PCR) ($p = 0.0001$). These results suggest that *mammaglobin* could be a marker of axillary lymph node breast metastases. Copyright © 1999 John Wiley & Sons, Ltd.

KEY WORDS—breast cancer; tumour progression; *mammaglobin*; uteroglobin; metastasis; marker; lymph node; subtractive hybridization

INTRODUCTION

The detection of breast cancer metastases and micrometastases based on specific genetic markers may provide useful information to guide early therapeutic decisions.¹ Various biological markers have been proposed for the detection of breast cancer cells, including *Keratin-19* and *Muc-1*,² but the frequency of expression of these markers is often related to tumour differentiation and is not always confined to breast tissue.³ This relates in part to the fact that most potential markers are derived initially from the study of other tissues and systems.

In order better to understand the molecular alterations that are specifically involved in breast tumour progression and that might provide molecular targets for detection, we and others have undertaken direct studies of human breast tumours. These studies aim to identify genes differentially expressed between normal and neoplastic tissue, or between different components of the same human breast tumour.^{4–6} *Mammaglobin*, a member of the uteroglobin gene family, has recently been identified by this approach as a gene that is overexpressed in breast tumours.⁷ In this study, we have also identified *mammaglobin* mRNA as being differentially expressed between the non-invasive *in situ* and

invasive components of a single breast tumour. We have gone on to investigate the cellular origin *in vivo* and the pattern of expression of *mammaglobin* mRNA in relation to tumour progression within primary tumours and their nodal metastases by *in situ* hybridization and reverse transcription-polymerase chain reaction (RT-PCR).

MATERIALS AND METHODS

Human breast tissues

All breast tumour cases were selected from the NCIC-Manitoba Breast Tumour Bank (Winnipeg, Manitoba, Canada). As previously described, all cases in the bank have been processed to create formalin-fixed and paraffin-embedded tissue blocks and mirror-image frozen tissue blocks.⁸ Histopathological analysis has been performed on haematoxylin and eosin (H&E) stained paraffin sections from the former block in each case to determine the tumour type, tumour grade (Nottingham system),⁹ and the distinction between *in situ* and invasive elements. Steroid receptor status has been determined for all cases by ligand binding assay performed on an adjacent portion of tumour tissue. Tumours with oestrogen and progesterone receptor levels below 3 and 10 fmol/mg of total protein, respectively, were considered ER- or PR-negative. Three groups of cases were used in this study as detailed below.

The initial 'microdissection case' consisted of a single tumour (No. 2, Table I) with extensive *in situ* lobular and limited (<25 per cent) invasive lobular components.

*Correspondence to: Etienne Leygue, PhD, Department of Biochemistry and Molecular Biology, University of Manitoba, 770 Bannatyne Avenue, Winnipeg, MB R3E 0W3, Canada. E-mail: eleygue@cc.umanitoba.ca

Contract/grant sponsor: Canadian Breast Cancer Research Initiative (CBCRI).

Contract/grant sponsor: U.S. Army Medical Research and Materiel Command (USAMRMC).

Table I—Clinical and pathological features of the breast tumours studied for *mamaglobin* mRNA expression by *in situ* hybridization*

No.	Mamaglobin score				Tumour characteristics					
	Normal ducts/lobules	<i>In situ</i> carcinoma	Invasive carcinoma	Nodal metastasis	Tumour type	Age (years)	Grade	ER	PR	NS
1	0·0 (0·0 × 0·0)	0·1 (1·0 × 0·1)	0·0 (0·0 × 0·0)	0·1 (1·0 × 0·1)	Ductal NOS	56	II	47	4·9	+
2	0·2 (2·0 × 0·1)	1·5 (3·0 × 0·5)	0·0 (0·0 × 0·0)	1·0 (2·0 × 0·5)	Lobular	45	II	3·5	28	+
3	0·1 (1·0 × 0·1)	0·2 (2·0 × 0·1)	0·0 (0·0 × 0·0)	na	Lobular	75	I	7·4	9·1	—
4	0·1 (1·0 × 0·1)	0·5 (1·0 × 0·5)	0·1 (1·0 × 0·1)	0·2 (2·0 × 0·1)	Ductal NOS	48	III	0·6	2·2	+
5	0·2 (2·0 × 0·1)	2·0 (2·0 × 1·0)	1·0 (1·0 × 1·0)	2·0 (2·0 × 1·0)	Lobular	58	II	37	15·9	+
6	0·1 (1·0 × 0·1)	0·1 (1·0 × 0·1)	1·0 (2·0 × 0·5)	1·5 (3·0 × 0·5)	Ductal NOS	63	II	1·8	12·2	+
7	0·2 (2·0 × 0·1)	0·2 (2·0 × 0·1)	2·0 (2·0 × 1·0)	na	Lobular	70	I	9·2	53	—
8	0·0 (1·0 × 0·0)	2·0 (2·0 × 1·0)	3·0 (3·0 × 1·0)	3·0 (3·0 × 1·0)	Lobular	48	I	10·3	7·2	+
9	0·0 (0·0 × 0·1)	2·0 (2·0 × 1·0)	3·0 (3·0 × 1·0)	na	Ductal NOS	72	III	32	46	—
10	0·1 (1·0 × 0·1)	0·1 (1·0 × 0·1)	3·0 (3·0 × 1·0)	2·0 (2·0 × 1·0)	Duct-Lob mix	44	II	0·6	27	+
11	0·0 (0·0 × 0·0)	0·0 (0·0 × 0·0)	0·0 (0·0 × 0·0)	0·0 (0·0 × 0·0)	Ductal NOS	80	II	1	8·5	+
12	0·5 (1·0 × 0·5)	0·0 (0·0 × 0·0)	0·0 (0·0 × 0·0)	0·0 (0·0 × 0·0)	Ductal NOS	36	II	22	42	+
13	0·2 (2·0 × 0·1)	0·0 (0·0 × 0·0)	0·0 (0·0 × 0·0)	na	Ductal NOS	32	II	5·8	41	+

*No=case number. The level of *mamaglobin* expression within normal ducts and lobules, *in situ* tumour, invasive tumour, and nodal metastasis components in each case is indicated by an overall score (shown in bold) derived from the product of the average signal intensity × the proportion of positive epithelial cells in each region (shown in parentheses) as described in the Materials and Methods section. Tumour type: ductal NOS=invasive ductal carcinoma; lobular=invasive lobular carcinoma; duct-lob mix=mixed invasive ductal and invasive lobular carcinoma. Grade: Nottingham grade score. ER/PR: oestrogen and progesterone receptor levels in fmol/mg total protein. na: not available. NS: axillary nodal status. +=node-positive; —=node-negative.

For the *in situ* hybridization studies, a series of 13 tumours was selected that contained normal ducts and lobules, and *in situ* and invasive tumour components, within a single section. For nine of these cases, axillary lymph node metastases were also available and these tissue blocks were analysed simultaneously. The histological features are summarized in Table I. These cases, which included the initial microdissection case, comprised invasive ductal ($n=7$), invasive lobular ($n=5$), and invasive mixed duct and lobular ($n=1$) carcinoma types. The tumour grades ranged from high (grade III, $n=2$), through intermediate (grade II, $n=8$), to low (grade I, $n=3$), and the steroid receptor status included both ER-positive ($n=9$) and ER-negative cases ($n=4$).

For the RT-PCR analysis studies of *mamaglobin* expression, a second panel of 20 primary breast tumours and their corresponding axillary nodes was selected. This panel included 13 node-positive tumours and seven node-negative tumours and in each case, the nodal status (i.e. absence, lymph node-negative; or presence, lymph node-positive) of the frozen tissue lymph node block that was used for this analysis was determined by histological analysis of H&E-stained sections from the adjacent mirror-image formalin-fixed and paraffin-embedded block. In this series, 18 cases were invasive ductal and two were invasive lobular carcinomas and the majority were high ($n=7$) or intermediate ($n=11$) grade, and ER-positive ($n=16$).

Subtractive hybridization analysis

The microdissection of the initial single tumour case was performed as previously described.⁸ After extraction

of total RNA, the subtractive hybridization was performed as previously described, using the *in situ* and the invasive component of the initial microdissection case as the tester and the driver, respectively.⁴

In situ hybridization

Paraffin-embedded 5 µm breast tumour sections were analysed by *in situ* hybridization according to a previously described protocol.⁵ The plasmid Mam-503, which consisted of PCR[®]II plasmid (Invitrogen, San Diego, CA, U.S.A.), containing a 503 bp insert of *mamaglobin* cDNA between bases 1 and 503,⁷ was used as a template to generate [³⁵S] UTP-labelled sense and antisense riboprobes using Riboprobe[®] Systems (Promega, Madison, WI, U.S.A.) according to the manufacturer's instructions. Sections were then developed and counterstained with H&E after 15 days. Levels of *mamaglobin* expression were assessed in normal, *in situ*, invasive, and, when possible, nodal metastatic regions by bright-field microscopic examination at low magnification and using a previously described semiquantitative approach.¹⁰ Scores were obtained for each component by estimating the average signal intensity (on a scale of 0–3) and the proportion of epithelial cells showing a positive signal (0, none; 0·1, less than one-tenth; 0·5, less than one-half; 1·0 greater than one-half). The intensity and proportion scores were then multiplied to give an overall score. Statistical comparisons between matched compartments were performed using the two-tailed Wilcoxon signed rank test. The correlation between *mamaglobin* expression within the invasive component and the corresponding nodal metastasis was established

by calculation of the Spearman rank correlation coefficient.

RT-PCR analysis

One microgram of total RNA was reverse-transcribed in a final volume of 20 μ l and 1 μ l of the reaction mixture subsequently amplified by PCR as previously described.⁵ The primers used corresponded to *mammaglobin* (sense, exon 1, 5'-CCGACAGCAGCAGCC TCAC-3', located in the *mammaglobin* sequence between bases 41 and 59⁷ and antisense, exon 3, 5'-TCCGT AGTTGGTTTCTCAC-3', located in the *mammaglobin* sequence between bases 401 and 383⁷) and to the ubiquitously expressed glyceraldehyde-3-phosphate dehydrogenase (*GAPDH*) gene (sense 5'-ACCCACTCCTC CACCTTTG-3' and antisense 5'-CTCTTGCTCTT GCTGGG-3'). To amplify cDNA corresponding to *mammaglobin* and *GAPDH*, 30 cycles (30 s at 94°C, 30 s at 55°C, and 30 s at 72°C) of PCR were used. Ten microlitres of *mammaglobin* PCR and *GAPDH* PCR were mixed and analysed by electrophoresis on prestained (ethidium bromide, 15 μ g/ml) 2 per cent agarose gels. The identity of the expected 361 bp long fragment corresponding to *mammaglobin* was confirmed by sequencing. Association between *mammaglobin* expression within nodal metastasis and histopathological determination of nodal status was tested using Fisher's exact test.

RESULTS

Identification of *mammaglobin* mRNA in breast cancer

A 'microdissection case' that contained lobular carcinoma *in situ* associated with invasive carcinoma was selected and frozen tissue blocks were subjected to microdissection to obtain material for extraction of total RNA corresponding to both regions.⁸ This RNA provided the substrate for a recently described subtractive hybridization technique.⁴ Upon completion of subtraction, a 503 bp long fragment was isolated as corresponding to a gene overexpressed in the *in situ* compartment (data not shown). Sequencing of this fragment identified nucleotides 1–503 of the sequence encoding *mammaglobin*, a recently described putative member of the uteroglobin family.⁷

Assessment of *mammaglobin* mRNA expression in normal breast tissue, *in situ* and invasive tumour elements and corresponding axillary lymph nodes

To establish which cells express *mammaglobin* mRNA within breast tumour tissues and to examine the distribution of the expression of this mRNA within different breast tumour components, 13 cases that included both lobular and ductal tumours were selected from the NCIC-Manitoba Breast Tumour Bank. For each case, the age of the patient and clinical characteristics of the tumour [i.e. Nottingham grade, oestrogen receptor (ER), progesterone receptor (PR) levels, as determined

by ligand binding assay, and nodal status] are given in Table I. Paraffin tissue sections containing normal ducts/lobules, *in situ* and invasive elements were studied by *in situ* hybridization, together (when available) with corresponding axillary lymph node paraffin sections (Fig. 1). No signal was detectable when a sense probe was used (Fig. 1A). In contrast, a signal varying in intensity was observed in epithelial cells when an antisense probe was used (Figs 1B–1D). *Mammaglobin* mRNA was not detected in stromal or inflammatory cells in any of the sections studied. Expression of *mammaglobin* was quantified in each component using a semi-quantitative approach described in the Materials and Methods section (Table I). Although *mammaglobin* mRNA was found to be overexpressed in the *in situ* tumour cells compared with normal adjacent epithelial cells in 7/13 cases, this difference did not reach statistical significance (Wilcoxon signed rank test, $n=9$, $p>0.05$). Similarly, even though *mammaglobin* expression appeared higher within the invasive component compared with normal adjacent elements in 6/13 cases, this difference was not statistically significant (Wilcoxon signed rank test, $n=10$, $p>0.05$). However, when both *in situ* and invasive elements were combined, *mammaglobin* expression observed in tumour was higher than that seen in normal adjacent cells (Wilcoxon signed rank test, $n=12$, $p<0.02$). This suggests that although *mammaglobin* mRNA is predominantly overexpressed in cancer cells within the primary tumour, the exact stage at which this increase in expression occurs varies between tumours and the nature of the alteration is complex. For example, when comparing matched *in situ* and invasive components, the *mammaglobin* mRNA level was found to be increased within *in situ* elements in 5/13 (40 per cent) cases (Table I, cases 1–5) but was increased within invasive elements in 5/13 (40 per cent) cases (Table I, cases 6–10) and was similar and low in 3/13 (20 per cent) cases (Table I, cases 11–13).

In nine cases, a paraffin tissue block from a synchronous nodal metastasis was also available for study. *Mammaglobin* expression was detectable within metastatic tumour cells in 7/9 cases and was undetectable only in the two cases where *mammaglobin* expression was absent in the primary tumour (Table I). This detection was possible in both early metastasis within the subcapsular sinus (Fig. 1C) and established metastasis (Fig. 1D). Evaluation of the level of *mammaglobin* mRNA expression within these lymph node metastases revealed a significantly (Wilcoxon signed rank test, $n=8$, $p<0.04$) higher level than that detected in matched normal breast tissue. The level of expression of *mammaglobin* mRNA within axillary lymph node metastatic cells was also found to correlate closely with the level observed within matched invasive elements (Spearman $r=0.89$, $p<0.002$).

Mammaglobin mRNA expression within the primary invasive tumour component appeared to be unrelated to several pathological indicators of tumour differentiation and prognosis. Expression was observed in both invasive ductal and lobular tumour types and increased expression showed no relation to tumour grade, the level of steroid receptors, or the presence or absence of nodal

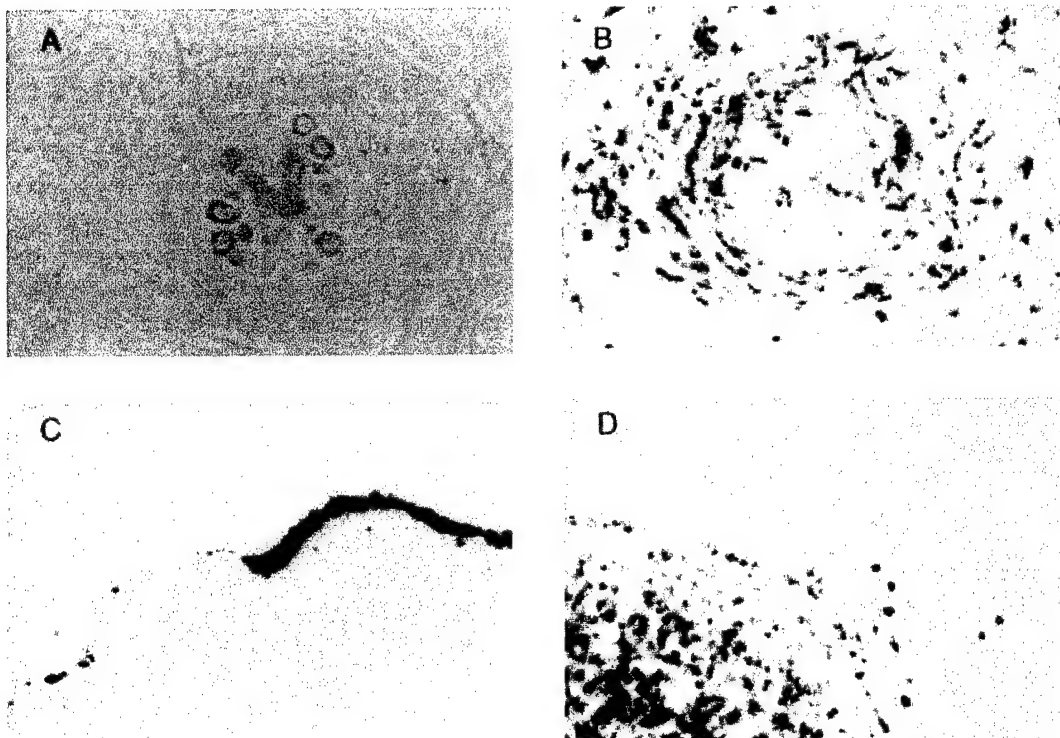


Fig. 1—Expression of *mammaglobin* mRNA in a primary breast tumour and concurrent nodal metastases (case 10, Table I) studied by *in situ* hybridization. Plates A and B illustrate consecutive sections from the primary tumour showing a normal lobular unit (in the middle) surrounded by invasive lobular carcinoma. Plate C shows a focus of early metastatic tumour confined to the subcapsular lymph node sinus. Plate D shows established nodal metastasis in an adjacent lymph node. (A) sense probe; (B, C, D) antisense probe

metastasis. Similarly, cases which showed an apparent reduction in the level of expression between *in situ* and invasive elements of the primary tumour showed no distinguishing features from those which showed the opposite changes.

Detection of *mammaglobin* mRNA expression in axillary nodal metastases

Because it was possible to detect *mammaglobin* mRNA in axillary lymph node metastases in seven out of nine metastases by *in situ* hybridization, and because this mRNA had previously been described as being absent from normal lymph node tissue,⁷ we investigated the possibility that *mammaglobin* could be a marker of axillary lymph node metastases. Twenty independent cases were selected, 13 axillary lymph node-positive and seven node-negative. Total RNA was extracted from frozen primary tumour sections and frozen node sections of corresponding axillary lymph nodes. The histological status of all tissues was confirmed in paraffin sections cut from adjacent mirror-image paraffin tissue blocks that had been processed in parallel to the frozen blocks.⁸ Total RNA was reverse-transcribed and analysed by RT-PCR using primers recognizing specifically *mammaglobin* cDNA and chosen to span intronic regions. PCRs were performed in triplicate with repro-

ducible results. The identity of the PCR product obtained was confirmed by sequencing. As shown in Fig. 2, no *mammaglobin* expression was detected in lymph nodes from cases without histologically detectable tumour cells (0/7 cases). In contrast, all lymph nodes previously identified to contain metastatic breast tumour cells following histopathological assessment had detectable *mammaglobin* expression (13/13 cases). The RT-PCR detection of *mammaglobin* mRNA in axillary lymph nodes appeared, therefore, strongly associated (Fisher's exact test, $p < 0.0001$) with the histopathological detection of lymph node metastases.

Consideration of the frequency of *mammaglobin* mRNA expression detectable by RT-PCR in this series (as opposed to *in situ* hybridization as performed in the first series) shows that 16/20 primary tumours were positive overall. The absence of signal in four cases could not be attributed to degraded RNA and/or cDNA, as shown by the amplification of the ubiquitously expressed *GAPDH* cDNA in the same cDNA samples. These *mammaglobin*-negative cases included ductal ($n=3$) and lobular ($n=1$) tumour types, both high ($n=3$) and intermediate grade ($n=1$) and ER-positive ($n=2$) and -negative ($n=2$) tumours. *Mammaglobin* was detected at a higher frequency in primary tumours that were node-positive (12/13 cases, 90 per cent) than in primary tumours that were node-negative (4/7 cases, 60

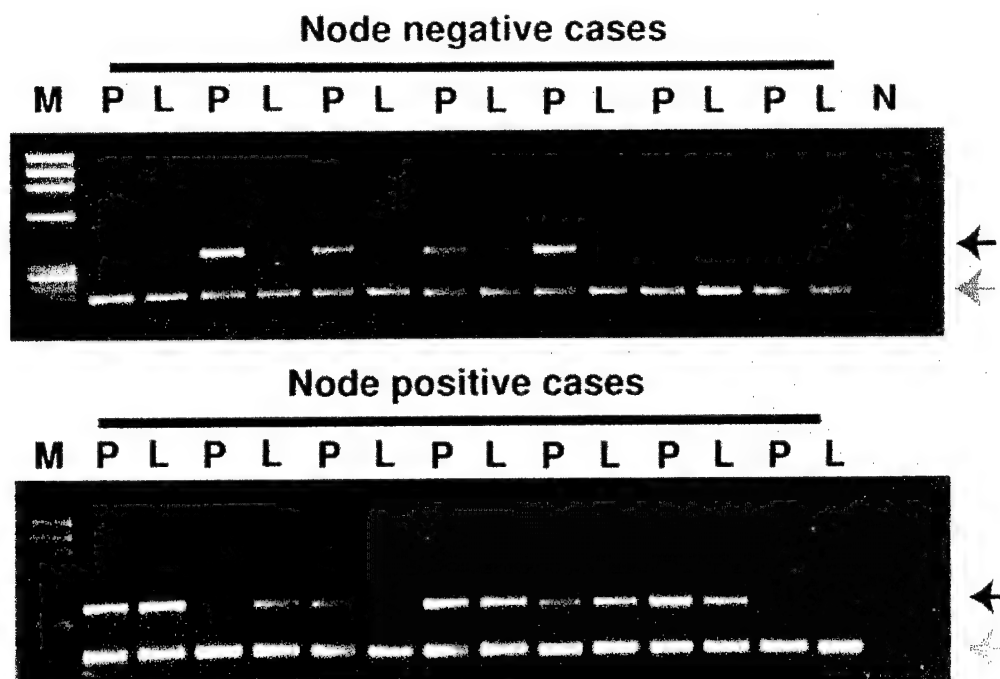


Fig. 2—RT-PCR analysis of *mammaplobin* and *GAPDH* mRNA expression in primary breast tumours (P) and their corresponding axillary lymph nodes (N) histologically shown to contain (node-positive) or not to contain (node-negative) metastases. PCR products were mixed before separation on 2 per cent agarose gels prestained with ethidium bromide. Black arrow: product corresponding to *mammaplobin*; grey arrow: product corresponding to *GAPDH*. M: Molecular weight marker (ϕ x174 RF DNA/Hae III fragments; Gibco BRL, Grand Island, NY, U.S.A.). N: Negative control; no cDNA added during the PCR.

per cent), although a similar trend was not seen in the initial series studied by *in situ* hybridization.

DISCUSSION

Mammaplobin has recently been identified as a breast-specific gene overexpressed by approximately 23 per cent of primary breast tumours.⁷ *Mammaplobin* is considered to be a member of the uteroglobin gene family and also maps to a region,¹¹ 11q13, that is frequently associated with alterations in breast tumorigenesis,^{12–18} but the cellular origin of expression of *mammaplobin* and the relationship between expression and tumour progression has not been previously determined. Our results show that the pattern of *mammaplobin* expression within breast tissues and tumour components is complex. Expression, is however, restricted to mammary epithelial cells, and in those tumours that show overexpression of *mammaplobin* in the invasive primary tumour, this expression appears invariably conserved in the concurrent axillary nodal metastases.

Mammaplobin was identified in the present study through detailed analysis of a single breast tumour to distinguish genes differentially expressed at early stages of tumour progression. The initial observation suggested that *mammaplobin* might be more highly expressed in the pre-invasive *in situ* than in the invasive elements of breast tumours. This is a pattern of expression that

would be consistent with data which suggest that expression of the uteroglobin can influence the invasiveness of epithelial tumour cells in other tissues.^{19,20} However, subsequent analysis revealed a more complex pattern of expression. In some cases (≈ 20 per cent), expression was undetectable by *in situ* hybridization at all stages; in some (≈ 40 per cent), the expression changed little, or even declined with progression from *in situ* to invasive disease; and in others (≈ 40 per cent), the expression increased. We also found that *mammaplobin* mRNA expression, measured by either *in situ* hybridization or RT-PCR in the primary tumours, was unrelated to tumour type, grade, or steroid receptor levels, as has been previously reported.^{7,11}

This complexity in expression may be related to the fact that the *mammaplobin* gene is localized to a chromosomal region, 11q13, that has been previously shown to be commonly modified during breast tumorigenesis. Alterations at this locus include loss of heterozygosity at markers adjacent to and on either side of the *mammaplobin* gene (*Pygm* and *Int-2*) occurring at increasing frequencies (from 9 per cent up to 67 per cent of informative cases) in association with progression from atypical ductal hyperplastic breast lesions, through lobular and ductal *in situ* neoplastic lesions, to invasive breast cancer.^{12,13,18} Amplification of the 11q13 region that includes several known genes such as *int-2*, *cyclin D1* and *ems-1* has also been observed in up to 15 per cent of invasive breast carcinomas,^{14–17} although the

amplified region may not directly involve the *mammaglobin* gene. The possible role of 11q13 modifications in the differential expression of the *mammaglobin* gene between normal and malignant breast tissue thus remains to be addressed.

In the course of our own molecular studies, even though based on the careful microdissection of regions containing a majority of epithelial cells, we have identified genes expressed only by epithelial cells,⁵ only by fibroblastic cells,¹⁰ or by both tumour and stromal cell types (our unpublished data). Therefore, the determination of the epithelial cellular origin and range of tumour components that express a particular gene *in vivo*, as opposed to within established cell lines, is of crucial importance if we are to understand the molecular functions of encoded proteins and their potential applications as tumour cell markers.

Given the previous suggestion that *mammaglobin* expression is restricted to breast tissues,⁷ we have examined the potential of this gene to be a marker of breast metastasis within axillary lymph nodes. Using RT-PCR, it was possible to detect *mammaglobin* in 13 out of 13 sections from axillary lymph nodes shown by histopathological examination of adjacent paraffin sections to contain metastatic cells and in none of seven nodes that were negative. The increased frequency of detection of *mammaglobin* in breast tumour cells using RT-PCR (primary 16/20 cases, 80 per cent; metastasis 13/13 cases, 100 per cent), compared with *in situ* hybridization (primary 10/13 cases, 77 per cent; metastasis 7/9 cases, 77 per cent) or northern blot (primary 23 per cent) as used by others,⁷ is most likely due to differences in sensitivity between assays.

The physiological role of *mammaglobin* in breast tissue is unknown, as is its possible involvement in breast tumorigenesis. Our data suggest, however, that *mammaglobin* gene expression is modified during breast tumorigenesis and that it may be a good candidate marker for the detection and characterization of breast cancer metastasis.

ACKNOWLEDGEMENTS

This work was supported by grants from the Canadian Breast Cancer Research Initiative (CBCRI) and the U.S. Army Medical Research and Matériel Command (USAMRMC). The Manitoba Breast Tumour Bank is supported by funding from the National Cancer Institute of Canada (NCIC). PHW is a Medical Research Council of Canada (MRC) Clinician-

Scientist; LCM is an MRC Scientist; EL is a recipient of a USAMRMC Postdoctoral Fellowship; and TH-H is a recipient of an MRC studentship.

REFERENCES

1. Mori M, Mimori K, Inoue H, *et al*. Detection of micrometastases in lymph nodes by reverse transcriptase-polymerase chain reaction. *Cancer Res* 1995; **55**: 3417-3420.
2. Noguchi S, Aihara T, Motomura K, Imaoka S, Koyama H. Detection of breast cancer micrometastases in axillary lymph nodes by means of reverse transcription-polymerase chain reaction. Comparison between *Muc-1* mRNA and *Keratin-19* mRNA amplification. *Am J Pathol* 1996; **148**: 649-656.
3. Dingemans AM, Brakenhoff RH, Postmus PE, Giaccone G. Detection of cytokeratin-19 transcripts by reverse transcription-polymerase chain reaction in lung cancer cell lines and blood lung cancer patients. *Lab Invest* 1997; **77**: 213-220.
4. Leygue E, Watson PH, Murphy LC. Identification of differentially expressed genes using minute amount of RNA. *Biotechniques* 1996; **21**: 1008-1012.
5. Leygue E, Snell L, Hiller T, *et al*. Differential expression of psoriasin mRNA between *in situ* and invasive human breast carcinoma. *Cancer Res* 1996; **56**: 4606-4609.
6. Watson MA, Flemming TP. Isolation of differentially expressed sequence tags from human breast cancer. *Cancer Res* 1994; **54**: 4598-4602.
7. Watson MA, Fleming TP. Mammaglobin, a mammary-specific member of the uteroglobin gene family, is overexpressed in human breast cancer. *Cancer Res* 1996; **56**: 860-865.
8. Hiller T, Snell L, Watson PH. Microdissection/RT-PCR analysis of gene expression. *Biotechniques* 1996; **21**: 38-44.
9. Elston CW, Ellis IO. Pathological prognostic factors in breast cancer. *Histopathology* 1991; **19**: 403-410.
10. Leygue E, Snell L, Hiller T, *et al*. Expression of lumican in human breast carcinoma. *Cancer Res* 1998; **58**: 1348-1352.
11. Watson MA, Darrow C, Zimonjic DB, Popescu NC, Fleming TP. Structure and transcriptional regulation of the human mammaglobin gene, a breast cancer associated member of the uteroglobin gene family localized to chromosome 11q13. *Oncogene* 1998; **16**: 817-824.
12. Chuquai RF, Zhuang Z, Emmert-Buck MR, Liotta LA, Merino MJ. Analysis of loss of heterozygosity on chromosome 11q13 in atypical ductal hyperplasia and *in situ* carcinoma of the breast. *Am J Pathol* 1997; **150**: 297-303.
13. Nayar R, Zhuang Z, Merino MJ, Silverberg SG. Loss of heterozygosity on chromosome 11q13 in lobular lesions of the breast using microdissection and polymerase chain reaction. *Hum Pathol* 1997; **28**: 277-282.
14. Fantl V, Richards MA, Smith R, *et al*. Gene amplification on chromosome 11q13 and estrogen receptor status in breast cancer. *Eur J Cancer* 1990; **26**: 423-429.
15. Bieche I, Lidereau R. Genetic alterations in breast cancer. *Genes Chromosome Cancer* 1995; **14**: 227-251.
16. Courjal F, Cuny M, Simony-Lafontaine J, *et al*. Mapping of DNA amplifications at 15 chromosomal localizations in 1875 breast tumours: definition of phenotypic groups. *Cancer Res* 1997; **57**: 4360-4367.
17. Driouch K, Champeme MH, Beuzelin M, Bieche I, Lidereau R. Classical gene amplifications in human breast cancer are not associated with distant solid metastases. *Br J Cancer* 1997; **76**: 784-787.
18. Kerangueven F, Noguchi T, Coulier F, *et al*. Genome-wide search for loss of heterozygosity shows extensive genetic diversity of human breast carcinomas. *Cancer Res* 1997; **57**: 5469-5774.
19. Kundu GC, Mantile G, Miele L, Cordella-Miele E, Mukherjee AB. Recombinant human uteroglobin suppresses cellular invasiveness via a novel class of high-affinity cell surface binding site. *Proc Natl Acad Sci USA* 1996; **93**: 2915-2919.
20. Leyton J, Manyak MJ, Mukherjee AB, Miele L, Mantile G, Patierno SR. Recombinant human uteroglobin inhibits the *in vitro* invasiveness of human metastatic prostate tumour cells and the release of arachidonic acid stimulated by fibroblast-conditioned medium. *Cancer Res* 1994; **54**: 3696-3699.

APPENDIX E

PSORIASIN (S100A7) EXPRESSION AND INVASIVE BREAST CANCER

Sahar Al-Haddad*, Zi Zhang*, Etienne Leygue†, Linda Snell*, Aihua Huang*, Yulian Niu*,
Tamara Hiller-Hitchcock*, Kate Hole*, Leigh C Murphy†, Peter H. Watson*.

Affiliations of authors: * Department of Pathology (S.A., Z.Z., L. S., A.H., Y.N., T.H-H., K. H., P.H.W.) and † Department of Biochemistry and Molecular Biology (E.L., L.C.M.), University of Manitoba, Faculty of Medicine, Winnipeg, Manitoba, Canada, R3E OW3.

Running title: Psoriasin (S100A7) expression in breast cancer.

Key words: Psoriasin, S100, breast cancer, tumor progression.

Footnotes:

1 This work was supported by grants from the Medical Research Council of Canada (MRC) and the U.S. Army Medical Research and Materiel Command (USAMRMC). The Manitoba Breast Tumor Bank is supported by funding from the National Cancer Institute of Canada (NCIC). P. H. W. is an MRC Clinician-Scientist, L. C. M. is an MRC Scientist, E. L. is a recipient of a USAMRMC Postdoctoral Fellowship. T. H-H is a recipient of an MRC studentship award.

2 Correspondence should be addressed to Dr Peter Watson at Department of Pathology, D212-770 Bannatyne Ave, University of Manitoba, Winnipeg, MB. R3E OW3, Canada. Phone: (204) 789 3435; Fax: (204) 789 3931; E-mail: pwatson@cc.umanitoba.ca.

3 The abbreviations used are: RT-PCR, reverse transcription-polymerase chain reaction; IHC, immunohistochemistry; ISH, in-situ hybridization; H&E, Hematoxylin/Eosin; ER, estrogen receptor; PR, progesterone receptor; GAPDH, glyceraldehyde-3-phosphate dehydrogenase; NS = not significant.

Abstract.

Alteration of Psoriasin (S100A7) expression has previously been identified in association with the transition from pre-invasive to invasive breast cancer. In this study we have examined psoriasin mRNA and protein expression in relation to prognostic factors in a cohort of 57 invasive breast tumors, comprising 34 invasive ductal carcinomas and 23 other invasive tumor types (lobular, mucinous, medullary, tubular). We first developed an IgY polyclonal chicken antibody and confirmed specificity for psoriasin by Western blot and immunohistochemistry in transfected cells and tumors. The protein was also localized by immunohistochemistry to epithelial and stromal cell cytoplasm as well as nuclei in psoriatic skin and breast tumors, however in-situ hybridization showed that psoriasin mRNA expression was restricted to epithelial cells. In tumors, higher levels of psoriasin measured by RT-PCR and Western blot (93% concordance) were significantly associated with ER and PR negative status ($p < 0.0001$, $p = 0.0003$), and with nodal metastasis in invasive ductal tumors ($p = 0.035$), but not with tumor type or grade. Psoriasin expression also correlated with inflammatory infiltrates (all tumors excluding medullary, $p = 0.0022$). These results suggest that psoriasin may be a marker of aggressive behaviour in invasive tumors and are also consistent with a function as a chemotactic factor.

Introduction

Earlier diagnosis of breast cancer has increased the need for identification of molecular alterations that might serve as tissue markers to predict the risk of progression to metastatic disease. Amongst the most important of these alterations are likely to be those associated with the development of the invasive phenotype and the transition from pre-invasive to invasive cancer with the capability for subsequent metastasis.

We have recently identified psoriasin, (S100A7) as a gene that is frequently overexpressed in pre-invasive ductal carcinoma in situ (DCIS) relative to adjacent invasive carcinoma, suggesting a role in breast tumor progression ¹. Other members of the S100 gene family of calcium binding proteins have been implicated in a range of biological processes including tumor metastasis ². In particular, S100A2 has been shown to be downregulated in breast tumor cells relative to their normal epithelial cell counterparts ³, while upregulation of S100A4 has been strongly implicated in breast tumor metastasis ⁴⁻⁶. In the latter case this may reflect the ability of S100A4 to influence cell motility ⁷, the cytoskeleton ^{6, 8, 9} or cell adhesion molecules ¹⁰.

Psoriasin was initially identified as a highly abundant protein, belonging to the S100 gene family ¹¹, expressed by abnormally proliferating keratinocytes in psoriatic epidermis ^{12, 13}. It has subsequently been shown to be a secreted protein that can exert an effect as a chemotactic factor for inflammatory cells ^{14, 15}. However the function of psoriasin in breast cancer remains to be determined ¹⁶. In this study we have developed a psoriasin specific antibody and evaluated psoriasin expression in invasive breast tumors with different invasive and metastatic potential as well as host inflammatory response.

Materials and Methods

Human breast tissues and cell lines

All breast tumor cases used for this study were selected from the NCIC-Manitoba Breast Tumor Bank (Winnipeg, Manitoba, Canada). As has been previously described ¹⁷, tissues are accrued to the Bank from cases at multiple centers within Manitoba, rapidly collected and processed to create matched formalin-fixed-embedded and frozen tissue blocks for each case with the mirror image surfaces oriented by colored inks. The histology of every sample in the Bank is uniformly interpreted by a pathologist in Hematoxylin/Eosin (H&E) stained sections from the face of the paraffin tissue block. This information is available in a computerized database along with relevant pathological and clinical information and was used as a guide for selection of specific paraffin and frozen blocks from cases for this study. For each case interpretations included an estimate of the cellular composition (including the percentage of invasive epithelial tumor cells, collagenous stroma and fatty stroma), tumor type and tumor grade for ductal tumors (Nottingham score) ^{18, 19}. The inflammatory host response was scored semi-quantitatively on a scale of 1(low) to 5(high). Steroid receptor status was determined for all cases by ligand binding assay performed on an adjacent portion of tumor tissue. Tumors with estrogen and progesterone receptor levels above 20 fmol/mg and 15 fmol/mg of total protein respectively were considered ER or PR positive.

Two cohorts of tumors were selected. The first cohort comprised 35 invasive ductal carcinomas selected to include 6 subgroups differing in respect to estrogen receptor status (ER positive and ER negative) and tumor grade (low, intermediate, high). Additional selection criteria also included high tissue quality, presence of invasive tumor within >35% of the cross section of the frozen block for invasive ductal cases, and minimal (<5%) normal or in-situ epithelial components. The second cohort comprised 23 invasive tumors selected to include 4 subgroups of different tumor types ¹⁸ that vary in differentiation and metastatic potential including invasive lobular (6), medullary (5), tubular (6), and colloid (6). Similar secondary criteria were also used for this cohort.

For analysis of antibody specificity and for positive controls for tumor assays, MCF7 human breast cancer cells obtained from the ATCC were used. MCF7 cells were grown as previously described under normal conditions in the presence of 5% fetal bovine serum, to provide a negative control ²⁰.

Alternatively MCF7 cells were subjected to estrogen deprived conditions in the presence of charcoal-stripped serum prior to stimulation by estradiol (10^{-8} M) for 48 hours prior to harvesting to induce psoriasin expression and provide a positive control. As an additional positive control MDA-MB-231 human breast cancer cells were transfected with a plasmid containing the CMV promoter-adjacent to the psoriasin cDNA (manuscript in preparation) and stable transfectants (CL7FD3 cell clone) expressing psoriasin mRNA were also used.

Antibody Reagents.

A psoriasin specific chicken IgY polyclonal antibody was generated by immunization of chickens with a 14 amino acid peptide corresponding to the carboxy terminus of psoriasin (KQSHGAAPCSGGSQ, Bionostics, Toronto, and Aves Labs, Inc, Oregon). A >90% pure IgY fraction from chicken egg yolk, was obtained in PBS and then further purified by passing it over a psoriasin peptide affinity column made by binding the synthetic peptide to NHS-activated Sepharose 4B (Pharmacia Biotech), according to the manufacturer's instructions. The bound IgY was then eluted with 5.0 M Sodium thiocyanate., followed by dialysis against 2 changes of PBS. Additional antibodies used included a commercial anti-S100 antibody (Sigma) as well as another anti-psoriasin sheep polyclonal antibody generated by using the same carboxy terminus synthetic peptide in sheep (Bionostics), and a rabbit polyclonal antibody, raised against the recombinant protein (kindly provided by Prof. J. Celis, University of Aarhus, Denmark).

Western Blot Analysis

For tumors, multiple sections (10-20 x 20 μ m) were cut from the face of frozen tissue blocks immediately adjacent to the face of the matching paraffin block ¹⁷. For cell lines, trypsinized cell pellets were obtained from breast cancer cell lines (grown to ~80% confluence). Total protein lysates were extracted from both the cell-line pellets and frozen tissue sections, using Tri-reagent (Sigma), as described by the manufacturer. The recovered protein was dissolved in SDS-Isolation Buffer (50 mM Tris, pH 6.8, 20 mM EDTA, 5% SDS, 5 mM β -glycerophosphate, and a cocktail of protease inhibitors (Boehringer Mannheim). Protein concentrations were determined using the Micro-BCA Protein assay kit (Pierce). Sixty μ g of total protein lysates were run on a 16.5% SDS-PAGE mini gel, using Tricine SDS-PAGE to separate the proteins ²¹ and then transferred to

0.2 µm Nitrocellulose (Bio-Rad). After blocking in 10% skimmed milk powder in TBS-0.05% Tween (TBST buffer), blots were incubated with, chicken IgY anti-psoriasin antibody (~15 µg/ml in TBST), followed by incubation with secondary antibody, rabbit IgG anti-chicken IgY - conjugated to HRP (1:5000 dilution in TBST, Jackson ImmunoResearch Laboratories, Inc), and visualization by incubation with Supersignal (Pierce) as per manufacturer's instructions. Exposed x-ray films were photographed and the band intensities determined by video-image analysis, using MCID M4 software (Imaging Research, St. Catherine's, Ont.). All signals were adjusted with reference to the psoriasin transfected MDA-MB-231 cell control (CL7FD3), run on each blot.

Immunohistochemistry

Immunohistochemistry was performed on 5 µm paraffin embedded breast tumor tissue sections from tissue blocks fixed in 10% neutral buffered formalin for 18 to 24 hours. After deparaffinizing, clearing and hydrating to PBS buffer (Phosphate Buffered Saline, pH 7.4) containing 0.05% Tween 20 (Mallinckrodt), the sections were pre-treated with hydrogen peroxide (3%) for 10 minutes to remove endogenous peroxidases and non-specific binding was blocked with normal rabbit serum (1:50, Sigma) to inhibit non-specific binding. Primary chicken IgY anti-psoriasin antibody (1:500 dilution in PBS) was applied for one hour at 37 °C followed by washing and incubation with the secondary antibody, peroxidase-conjugated affinity purified rabbit anti-chicken (1:200 dilution), for 1 hour at room temperature. Detection was performed with DAB peroxidase substrate (Sigma) and counterstaining with Methyl Green (2%), followed by dehydration, clearing and mounting. A positive tissue control and a negative reagent control (normal rabbit serum / no primary antibody) were run in parallel in all experiments. Immunostaining pattern and intensity were assessed by light microscopy and both parameters were scored using an H-score system as previously described ²².

In-situ hybridization

In-situ hybridization was performed on paraffin sections (5 micron) according to a previously described protocol ¹. Linearized psoriasin plasmid cDNA, 1.0 ug/ul was used to generate UTP^{S35} labelled sense and antisense RNA probes using the Riboprobe System (Promega, Madison, WI.) according to the manufacturer's instructions. Sense and antisense probes were equalized by diluting

1×10^6 cpm/ μ l in hybridization solution. These were then applied to paraffin sections (approximately 30 μ l of probe per section) that had undergone post-fixation with 4% paraformaldehyde, pH 7.4 in PBS and further pretreatments with triethanolamine/acetic anhydride and proteinase K prior to hybridization. Sections were then coverslipped, sealed and incubated overnight in a humid chamber at 42° C. After coverslip removal, sections underwent incubation in post-hybridization solution and buffered Rnase A (20 μ g/ μ l), followed by several washes in descending dilutions of SSC buffer to remove weakly bound non-specific label. After dehydration in ethanol containing 300 mM ammonium acetate, the sections were coated in NTB-2 Kodak emulsion and subsequently developed after various time intervals from 2 to 5 weeks, and counterstained with Lee's Methylene Blue and Basic Fuchsin. Psoriasin expression was assessed by brightfield microscopic examination at low power (10x objective) magnification with reference to the negative sense and positive control tumor sections run with each batch. Levels were scored as previously described ²³ by assessing the average signal intensity (on a scale of 0 to 3) and the proportion of tumor cells showing a positive signal (0, none; 0.1, less than one tenth; 0.5, less than one half; 1.0 greater than one half). The intensity and proportion scores were then multiplied to give an overall score. Tumors with a score lower than 1.0 were deemed negative or weakly positive.

Reverse Transcriptase-Polymerase Chain Reaction (RT-PCR) Analysis.

RT-PCR was performed based on extracted RNA (600ng) that was reverse transcribed in a total volume of 20 μ l as described previously ¹. Briefly, reverse transcription completed using the following reaction mixture: for each sample, 200 ng (2 μ l of 0.1 μ g/ μ l) of total RNA was added to 16 μ l of RT mix (4 μ l of 5X RT buffer; 1 μ l of each dATP, dCTP, dGTP, and dTTP all at 2.5mM; 2 μ l of 0.1% BSA; 2 μ l of 0.1M DTT; 1 μ l of 0.25M random hexamer primer; 2 μ l of DMSO and 1 μ l of 200 units/ μ l of MMLV reverse transcriptase) and incubated at 37°C for 1.5 hours. Each PCR reaction was performed in a 50 μ l volume using 1 μ l of the completed RT reaction (cDNA); 30.8 μ l of sterile water; 5 μ l of 10X PCR buffer; 5 μ l of 25mM MgCl₂; 200 mM each of dATP, dCTP, dGTP and dTTP; 1 μ l of DMSO; 1 unit of Taq DNA polymerase and 0.5 μ l of 50 mM PCR primers. The psoriasin primers were sense (5'-AAG AAA GAT GAG CAA CAC -3') and antisense (5'-CCA GCA AGG ACA GAA ACT-3') corresponding to the cDNA sequence ¹³, or alternatively PCR was performed with GAPDH primers, sense (5'-ACC CAC TCC TCC ACC TTT G-3') and

antisense (5'- CTC TTG TGC TCT TGC TGG G-3')²⁴. For PCR amplification the reaction comprised an initial step of 5 minutes at 94°C, and then 45 cycles (30 seconds at 94°C, 30 seconds at 56°C, 30 seconds at 72°C) for psoriasin or 35 cycles (45 seconds at 93°C, 45 seconds at 58°C, 30 seconds at 72°C) for GAPDH. PCR products of the two genes amplified from the same RT reaction were loaded into the same wells onto a 1.5% agarose gel prior to electrophoresis and ethidium bromide staining in order to visualize psoriasin (246 bp) and GAPDH (198 bp) cDNAs under UV illumination.

Preliminary experiments were performed with cell line and tumor RNA samples to establish the appropriate RNA input and PCR cycle number conditions to achieve amplification with both psoriasin and GAPDH primers in the linear range in a typical sample. Tumors from each cohort were processed as a batch, from frozen sectioning to RNA extraction, reverse transcription in triplicate and then duplicate PCRs from each RT reaction. For each batch controls included RT- and RNA- controls, and both psoriasin positive (estradiol stimulated MCF7) and psoriasin negative (untransfected, wild type MDA-MB-231 cells) RNA controls. All primary tumor PCR signals were assessed in gels and autoradiographs by video image capture and MCID-M4 image analysis program. Psoriasin expression was standardized to GAPDH expression assessed from the same RT reaction in separate PCR reactions and run in parallel on the same gel, and the mean of each duplicate PCR then expressed relative to the levels in the MCF7 cell line standard. To correct for differences in processing between electrophoresis gels, psoriasin levels in each tumor were further standardized to a set of PCR product standards incorporated into each gel.

Statistical Analysis.

For analysis of associations, standardized psoriasin mRNA levels were used either as a continuous variable or transformed into low or high expression categories using a level of 1 relative density units. This cutpoint was selected to correspond to the lowest level at which protein could be detected by Western blot. Correlations with ER and PR levels and inflammation were tested using Spearmans test. Associations with categorical variables were tested by either Mann Whitney or ANOVA tests for selected dependent variables, or un-paired t-test for independent variables, or Chi-squared test.

Results

Characterization of Psoriasin Specific Antibodies

Multiple S100 proteins are expressed in individual tissues and cells. To specifically distinguish psoriasin expression within archival formalin fixed and paraffin embedded tissues we raised a polyclonal antibody in chicken against a synthetic peptide that corresponded to the COOH terminus of psoriasin. This 14 amino acid region was selected on the basis of very low homology to other S100 proteins. Western blot analysis of an MDA-MB-231 breast cell line transfected with a plasmid incorporating psoriasin cDNA under the control of a CMV promotor (and known to express psoriasin mRNA by Northern blot, unpublished data) and breast tumors showed a single band corresponding to a protein of approx 11.5 kDa with the chicken IgY antibody (figure 1A). This signal could be inhibited by pre-incubation of the primary antibody with psoriasin synthetic peptide (data not shown), and was absent from the wild type and vector alone transfected MDA-MB-231 control cells. By comparison a commercial anti-S100 antibody (Sigma), known to detect several S100 proteins in MDA-MB-231 cells ²⁵, weakly recognized the same 11.5 kDa protein in transfected cells as well as several other S100 proteins in most samples (figure 1B). Both antibodies recognized additional higher molecular weight bands in most samples. However, specificity of the 11.5 kDa psoriasin signal was further confirmed by Western blot using another anti-psoriasin polyclonal antibody raised against the same peptide in sheep, and a third polyclonal anti-psoriasin rabbit antibody previously raised against a recombinant psoriasin protein (data not shown).

Localization of Cellular Expression of Psoriasin

To assess the ability of these antibodies to detect psoriasin in formalin-fixed paraffin embedded tissues we selected paraffin blocks from a set of 13 breast tumors that showed high (6 cases) or low (7 cases) levels of psoriasin mRNA expression (determined by RT-PCR analysis of RNA extracted from sections cut from the adjacent mirror image frozen tissue blocks as described below). Two independent skin biopsies from psoriatic lesions and a laryngeal squamous carcinoma were also selected as positive control tissues. All cases were subjected to both immunohistochemistry and in-situ hybridization on adjacent sections and both signals were assessed independently using a semi-quantitative scoring system and without reference to the RT-PCR results (Table 1). There was a

good correlation between IHC protein expression and mRNA expression determined by either RT-PCR ($r=0.84$, $p=0.0003$) or ISH ($r=0.59$, $p=0.035$), despite the presence of additional apparently non-specific bands detected by Western blot. Psoriasin protein signals in breast tumors were detected at different levels, predominantly within epithelial tumor cells but also within some adjacent inflammatory cells and in some cases also on the luminal aspects of endothelial cells within small vessels (figure 2). However, in-situ hybridization demonstrated that mRNA expression was limited to tumor cells (figure 2). An unexpected finding was that psoriasin protein appeared to be localized within both breast tumor cell nuclei as well as cytoplasm. Examination of skin biopsies showed that positive immunohistochemical staining was predominantly localized to keratinocytes within the mid to upper zones of the epidermis, corresponding to the cells that also showed mRNA expression by in-situ hybridization (figure 2). Positive immunohistochemical staining, but no mRNA signal, was also observed on the luminal aspect of endothelial cells lining small vessels with the underlying dermis. Psoriasin protein appeared to be localized to the cytoplasm within most keratinocytes, however in some areas of the epidermis strong nuclear staining was also observed, similar to the staining pattern seen in breast tumors (figure 2). The same nuclear and cytoplasmic localization was also detected in a squamous laryngeal carcinoma, and with the sheep anti-psoriasin antibody (data not shown). However the third polyclonal rabbit anti-psoriasin antibody previously shown to provide immunofluorescent staining in frozen skin sections ^{13, 26}, did not detect any signal on paraffin sections from skin or breast. Additional experiments were performed with the chicken IgY antibody on skin and breast tumor sections in which immunohistochemical conditions (microwave vs protease antigen retrieval) and tissue treatment / fixation conditions (formalin vs alcohol vs paraformaldehyde vs frozen) were varied, and nuclear localization persisted under all conditions (data not shown).

Expression of Psoriasin in Tumors

The changes in psoriasin expression previously observed in association with the transition from in-situ to invasive carcinoma suggested a functional role in early stages of progression. However, alteration of psoriasin expression in normal skin has also been associated with abnormal keratinocyte differentiation. To examine the relationship of psoriasin with differentiation and invasiveness further we examined psoriasin mRNA and protein levels in a cohort of invasive tumors that included several different tumor types and a range of differentiation as determined by

tumor grade and estrogen receptor status (Table 2). Psoriasin mRNA was detected in all tumors by RT-PCR, but the levels varied considerably (figure 3). Within the invasive ductal subgroup there was no significant difference in psoriasin expression with tumor grade. There was also no significant difference between tumor size or types, although there was a trend towards lower levels of expression in both well differentiated tumor types, tubular and mucinous carcinomas, while lobular and medullary carcinomas showed a trend towards higher expression than invasive ductal tumors. However higher levels of psoriasin mRNA expression showed a significant inverse correlation with both ER and PR levels ($r = -0.66$, $p=0.0001$; $r=-0.47$, $p=0.0003$ Spearman) and with ER and PR negative status (ER -ve vs +ve; $n=28$ vs 29 , mean^{sd} $1.032^{0.7}$ vs $0.32^{0.36}$, $p<0.0001$ Mann Whitney; PR -ve, $n=25$ vs 32 , $1.05^{0.72}$ vs $0.37^{0.40}$, $p<0.0001$) in all tumors and also within the invasive ductal subgroup. Psoriasin expression was also higher in axillary node positive cases in all tumors (mean^{sd} = $0.86^{0.73}$ vs $0.59^{0.66}$) and the difference was statistically significant for the invasive ductal subgroup (mean^{sd} = $0.88^{0.79}$ vs $0.38^{0.28}$, $p=0.035$ t-test). These relationships with ER, PR and nodal status (Table 3) were also evident and remained statistically significant after correction of psoriasin levels for the relative tumor cell content within the tissue sections studied.

As anticipated Western blot analysis was less sensitive and psoriasin protein was only detectable in 10 tumors (Table 2, figure 4). These tumors (6 ductal, 2 lobular, 2 medullary) corresponded to those with the highest mRNA levels observed by RT-PCR (above 1.0 arbitrary expression units). Also consistent with RT-PCR analysis, western blot positive invasive ductal tumors were also significantly associated with ER negative ($p<0.0001$) and PR negative ($p<0.0012$) and node positive ($p=0.0143$) status (Table 3).

The relationship between psoriasin expression and host inflammatory response was also examined (Table 3). This showed a significant positive correlation both in the entire cohort ($n=57$, $r=0.47$, $p=0.0002$), in the entire cohort excluding the medullary carcinoma subgroup, which includes inflammatory infiltrates as a diagnostic criterion ($n=52$, $r=0.42$, $p=0.0022$) and within the invasive ductal subgroup alone ($n=34$, $r=0.39$, $p=0.023$).

Discussion

We have developed a psoriasin specific antibody and confirmed its specificity as well as its ability to detect the psoriasin protein in formalin fixed and paraffin embedded specimens. We have shown that there is a high concordance between psoriasin mRNA and protein levels in invasive tumors and higher levels are significantly associated with poor prognostic markers including ER and PR negative and lymph node positive status. Psoriasin protein expression is also associated with inflammatory infiltrates.

Indirect support for a role for S100 genes in breast tumor progression is provided by several observations. Disruption of calcium signaling pathways has been implicated as a central mechanism in tumorigenesis and specifically in the process of invasion and metastasis ²⁷. Also the chromosomal location of the S100 gene family lies in a region of chromosome 1 that frequently (>50%) shows loss of heterozygosity in invasive tumors ²⁸. Furthermore, several S100 genes are expressed in breast cell lines and tumors and are known to manifest alteration of their expression in association with tumorigenesis and progression ^{25, 29}. In particular, S100A2 and S100A4 have been identified to be differentially expressed between normal and neoplastic cells ^{3, 30, 31} and upregulated in metastatic as compared to non-metastatic cells in both mouse and rat mammary tumor cell lines ^{5, 32}. In-vivo studies of breast tumors have also shown a correlation between high levels of S100A4 expression, nodal metastasis and ER negative status ³³. More direct evidence has emerged from modulation of S100A4 expression in transfected cell lines that have shown that overexpression of S100A4 can also induce the metastatic phenotype in mouse, rat and human cells ^{4, 6, 34}. Furthermore there is evidence that S100A4 may exert its effect on cell cytoskeleton ^{8, 9} and motility ⁷ and it has also been demonstrated that upregulation of S100A4 in mouse tumor cell lines can downregulate expression of E-cadherin and disturb the intracellular distribution of β -catenin ³⁵.

A possible role for psoriasin (S100A7) in breast cancer first emerged when it was also identified as a cDNA downregulated in a nodal metastasis relative to a primary breast tumor ³⁶. Nevertheless the significance of the initial observation was unclear because of the fact that expression was only detectable in a small proportion of cells within invasive primary tumors studied by in-situ

hybridization and overall could be detected in only 18% of primary tumor specimens assessed by Northern analysis. An explanation for this paradox became apparent when psoriasin was also identified by us as a gene that is particularly highly expressed in the ductal epithelial cells of pre-invasive ductal carcinoma-in-situ ¹, which can be present as a significant component with invasive tumor specimens. We have now shown that when higher levels of psoriasin expression persist within invasive tumors then this correlates with indicators of increased metastatic potential. It should be noted that the strong relationship with ER status is compatible with studies of S100A4 ³³ and also the in-vitro observation ³⁶ (and our unpublished data) that psoriasin is regulated by estradiol in MCF7 cells. Although it is interesting that the nature of this correlation is different between the in-vitro and in-vivo situations, suggesting that additional external factors may influence psoriasin regulation in-vivo.

While the biological effect of alteration of psoriasin in breast tumors is currently unknown, it is interesting to speculate from this pattern of expression that psoriasin may be important in the invasive phenotype ¹⁶. This role might be mediated through an indirect influence on the effector cells of the host immune response or perhaps through a more direct influence on the epithelial tumor cell. The first hypothesis is supported by the correlation seen here with the degree of host inflammatory cell response within breast tumors and the previous evidence that implicates psoriasin as a chemotactic factor ¹⁴. However, psoriasin protein was only detected in approximately 50% of medullary and ductal tumors with marked inflammatory responses. The second hypothesis is supported by our observation that psoriasin may not only be secreted ^{13, 15} but also can be localized in both nuclear and cytoplasmic compartments in normal skin and breast tumors. Although further studies beyond immunohistochemistry are necessary to confirm this assessment, several observations provide indirect support for multiple sites of localization. The pattern of expression is consistent between cells in two closely related epithelia, epidermis and breast ductal epithelium, and the detection of nuclear and cytoplasmic signal was unrelated to tissue fixation or IHC protocol, which may effect staining with some antibodies ^{37, 38}. Dual localization and alteration of this subcellular localization with disease has also been observed with another S100 related keratinocyte protein, profilaggrin, expressed in the epidermis ^{2, 39}, and altered cellular distribution of proteins such as BRCA1 and β -catenin is well recognized to be an important aspect of tumor progression ^{35, 40, 41}. Furthermore, other S100 proteins have previously been associated

with both extracellular and intracellular actions ⁴². For example, previous studies have also indicated potential interactions for S100A4 with both cytoskeletal ^{8, 9} and nuclear proteins ⁴³. Similarly, other secreted S100 proteins can be localized to cytoplasm and nucleus ^{44, 45} and specifically S100A2 has been found in breast cell nuclei while S100A6 localizes to the cytoplasm ²⁵, however the functional significance of these findings remains unknown.

In conclusion, we have shown that expression of psoriasin (S100A7) mRNA and protein correlates with indicators of poor prognosis in invasive breast tumors, including ER, PR, and nodal status, but is not related to differentiation as manifested by invasive tumor type or grade. The relationship observed between psoriasin and the inflammatory response is also compatible with a role as a chemotactic factor, however the possibility of additional intracellular functions is raised by the presence of its nuclear localization in both skin and breast tumors. Further studies will be necessary to confirm the latter observation and pursue the biological functions of psoriasin in relation to breast tumor progression.

Acknowledgements.

The authors thank Prof J.E. Celis (University of Aarhus, Denmark) for kindly providing anti-psoriasin antibody and Helmut Dotzlaw and Caroline Leygue-Cummins for assistance with cell transfections. We also thank Bionostics Inc, North York, Ontario for assistance with antibody production. The tissues used in this study were provided by the Manitoba Breast Tumor Bank, which is funded by the National Cancer Institute of Canada.

Figures

Figure 1. Western blot analysis of cell lines and tumors to demonstrate anti-psoriasin IgY antibody specificity. Panel A shows a protein band (approx 11.5 kDa) detected using a chicken IgY anti-psoriasin antibody in a psoriasin transfected MDA-MB-231 breast cell line and 2 tumors (10049, 12434) but absent in wild type MDA-MB-231 cells. Panel B shows detection of several S100 like proteins using a commercial polyclonal S100 antibody applied to the same samples, in addition to weak detection of the same (approx 11.5 kDa) protein band,.

Figure 2. Immunohistochemical and in-situ hybridization analysis of the cellular distribution and patterns of expression of psoriasin within psoriatic skin lesions and breast tumors. Psoriasin protein is localized in skin to both nuclei (A, white arrow) and cytoplasm (A, black arrow) of keratinocytes. Similar nuclear and cytoplasmic staining is seen in breast epithelial tumor cells (C, black arrow). Psoriasin protein is also detected within occasional stromal inflammatory cells (C, white arrow). Panel E shows an H&E stained section from the same region of the tumor shown in panel C. Psoriasin mRNA expression in skin is restricted to epithelial cells in suprabasal layers of epidermis (B) to scattered invasive epithelial tumor cells in breast tumors (D), detected using antisense probe (B & D) compared to sense probe (F). Original magnification for all panels at the microscope, x200.

Figure 3. RT-PCR analysis of psoriasin mRNA expression in invasive breast tumors. Psoriasin (upper black arrow) and GAPDH (lower open arrow) from duplicate PCRs of 10 representative tumors. Control lanes include estradiol treated MCF7-E2 cells, a tumor control 12077c, and wild type MDA-MB-231 cells.

Figure 4. Western blot analysis of psoriasin protein expression in invasive breast tumors. Psoriasin (black arrow) is detected in 3/12 tumors and within the positive control (MDAMB231 cells transfected with psoriasin cDNA).

Tables

Table 1. Comparison between psoriasin mRNA and protein expression in 13 cases assessed by RT-PCR, in-situ hybridization and immunohistochemistry.

Notes; TB# = tumor bank case #; RT-PCR = psoriasin mRNA level determined by RT-PCR; ISH score = psoriasin mRNA level determined by in-situ hybridization and semi-quantitative assessment of the intensity (int) and proportion (prop) as described in materials and methods); IHC = psoriasin protein level determined by immunohistochemistry and semi-quantitative assessment of the intensity (int) and proportion (prop) as described in materials and methods).

Table 2. Clinicopathological parameters, histological composition of the tumor section, and psoriasin expression in 57 invasive breast carcinomas assessed by RT-PCR and Western blot.

Notes; TB# = tumor bank case number; Type = mucinous (muc), tubular (tub), medullary (med), lobular (ilc), ductal (idc); ER, PR = estrogen/progesterone receptor levels, fmol/mg protein; GrSc = Nottingham grade score; size = tumor size, cms; NS = nodal status, positive (+), negative (-), not available (na); Inv%, IS%, N%, Str% = percentage of tissue section occupied by invasive tumor, in-situ tumor, normal ducts/lobules, collagenous and/or fat stroma; Inf = estimate of inflammatory infiltrate, low (1) to high (5). RT-PCR and RT/PCR/Inv% = psoriasin mRNA level determined by RT-PCR, both unadjusted and adjusted for the tumor cell content of the tissue section (as described in materials and methods); WB = psoriasin protein level determined by western blot (as described in materials and methods).

Table 3. Relationship between psoriasin expression and prognostic and tissue factors.

Notes; ER, PR = estrogen/progesterone receptor status; NS = nodal status; Inf = inflammatory infiltrate, Size = tumor size, cms, Grade = Nottingham grade; Type = mucinous (muc), tubular (tub), medullary (med), lobular (ilc), ductal (idc);. Low Ps/ High Ps = low / high psoriasin mRNA level determined by RT-PCR (cutpoint values used as described in materials and methods). P values determined by Chi-squared or ANOVA tests.

REFERENCES

1. Leygue E, Snell L, Hiller T, Dotzlaw H, Hole K, Murphy, LC, Watson, PH Differential expression of psoriasin messenger RNA between in situ and invasive human breast carcinoma. *Cancer Res* 1996;56:4606-4609.
2. Schafer BW, Heizmann CW. The S100 family of EF-hand calcium-binding proteins: functions and pathology. *Trends Biochem Sci* 1996;21:134-140.
3. Lee SW, Tomasetto C, Swisshelm K, Keyomarsi K, Sager R. Down-regulation of a member of the S100 gene family in mammary carcinoma cells and reexpression by azadeoxycytidine treatment. *Proc Natl Acad Sci U S A* 1992;89:2504-2508.
4. Lloyd BH, Platt-Higgins A, Rudland PS, Barraclough R. Human S100A4 (p9Ka) induces the metastatic phenotype upon benign tumour cells. *Oncogene* 1998;17:465-473.
5. Sherbet GV, Lakshmi MS. S100A4 (MTS1) calcium binding protein in cancer growth, invasion and metastasis. *Anticancer Res* 1998;18:2415-2421.
6. Grigorian M, Ambartsumian N, Lykkesfeldt AE, Bastholm, L, Elling F, Georgiev G, Lukanidin E. Effect of mts1 (S100A4) expression on the progression of human breast cancer cells. *Int J Cancer* 1996;67:831-841.
7. Ford HL, Salim MM, Chakravarty R, Aluiddin V, Zain SB. Expression of Mts1, a metastasis-associated gene, increases motility but not invasion of a nonmetastatic mouse mammary adenocarcinoma cell line. *Oncogene* 1995;11:2067-2075.
8. Kriajevska M, Tarabykina S, Bronstein I, Metastasis-associated Mts1 (S100A4) protein modulates protein kinase C phosphorylation of the heavy chain of nonmuscle myosin. *J Biol Chem* 1998;273:9852-9856.
9. Ford HL, Zain SB. Interaction of metastasis associated Mts1 protein with nonmuscle myosin. *Oncogene* 1995;10:1597-1605.
10. Keirsebilck A, Bonne S, Bruyneel E, Vermassen P, Lukanidin, E, Mareel, M, van Roy, F. E-cadherin and metastasin (mts-1/S100A4) expression levels are inversely regulated in two tumor cell families. *Cancer Res* 1998;58:4587-4591.
11. Hardas BD, Zhao X, Zhang J, Longqing X, Stoll S, Elder JT. Assignment of psoriasin to

human chromosomal band 1q21: coordinate overexpression of clustered genes in psoriasis. *J Invest Dermatol* 1996;106:753-758.

12. Hoffmann HJ, Olsen E, Etzerodt M, Madsen P, Thogersen H C, Kruse T, Celis J E. Psoriasin binds calcium and is upregulated by calcium to levels that resemble those observed in normal skin. *J Invest Dermatol* 1994;103:370-375.

13. Madsen P, Rasmussen HH, Leffers H, Honore B, Dejgaard K, Olsen E, Kiil J, Walbum E, Andersen A H, Basse B et al. Molecular cloning, occurrence, and expression of a novel partially secreted protein "psoriasin" that is highly up-regulated in psoriatic skin. *J Invest Dermatol* 1991;97:701-712.

14. Jinquan T, Vorum H, Larsen CG, Madsen P, Rasmussen H H, Gesser B, Etzerodt M, Honore B, Celis J E, Thestrup-Pedersen K. Psoriasin: a novel chemotactic protein. *J Invest Dermatol* 1996;107:5-10.

15. Celis JE, Rasmussen HH, Vorum H, Madsen P, Honore B, Wolf H, Orntoft T F. Bladder squamous cell carcinomas express psoriasin and externalize it to the urine. *J Urol* 1996;155:2105-2112.

16. Watson PH, Leygue ER, Murphy LC. Psoriasin (S100A7). *Int J Biochem Cell Biol* 1998;30:567-571.

17. Hiller T, Snell L, Watson PH. Microdissection RT-PCR analysis of gene expression in pathologically defined frozen tissue sections. *Biotechniques* 1996;21:38-40, 42, 44.

18. Ellis IO, Galea M, Broughton N, Locker A, Blamey RW, Elston CW. Pathological prognostic factors in breast cancer. II. Histological type. Relationship with survival in a large study with long-term follow-up. *Histopathology* 1992;20:479-489.

19. Elston CW, Ellis IO. Pathological prognostic factors in breast cancer. I. The value of histological grade in breast cancer: experience from a large study with long-term follow-up. *Histopathology* 1991;19:403-410.

20. Leygue ER, Watson PH, Murphy LC. Estrogen receptor variants in normal human mammary tissue. *J Natl Cancer Inst* 1996;88:284-290.

21. Schagger H, von Jagow G. Tricine-sodium dodecyl sulfate-polyacrylamide gel electrophoresis for the separation of proteins in the range from 1 to 100 kDa. *Anal Biochem*

1987;166:368-379.

22. Huang A, Pettigrew NM, Watson PH. Immunohistochemical assay for oestrogen receptors in paraffin wax sections of breast carcinoma using a new monoclonal antibody. *J Pathol* 1996;180:223-227.
23. Leygue E, Snell L, Dotzlaw H, Hole K, Hiller-Hitchcock T, Roughley P J, Watson P H, Murphy L C. Expression of lumican in human breast carcinoma. *Cancer Res* 1998;58:1348-1352.
24. Ercolani L, Florence B, Denaro M, Alexander M. Isolation and complete sequence of a functional human glyceraldehyde-3- phosphate dehydrogenase gene. *J Biol Chem* 1988;263:15335-15341.
25. Ilg EC, Schafer BW, Heizmann CW. Expression pattern of S100 calcium-binding proteins in human tumors. *Int J Cancer* 1996;68:325-332.
26. Ostergaard M, Rasmussen HH, Nielsen HV, Vorum H, Orntoft, T F, Wolf, H, Celis J. E. Proteome profiling of bladder squamous cell carcinomas: identification of markers that define their degree of differentiation. *Cancer Res* 1997;57:4111-4117.
27. Kohn EC, Liotta LA. Molecular insights into cancer invasion: strategies for prevention and intervention. *Cancer Res* 1995;55:1856-1862.
28. Munn KE, Walker RA, Varley JM. Frequent alterations of chromosome 1 in ductal carcinoma in situ of the breast. *Oncogene* 1995;10:1653-1657.
29. Borglum AD, Flint T, Madsen P, Celis JE, Kruse TA. Refined mapping of the psoriasin gene S100A7 to chromosome 1cen-q21. *Hum Genet* 1995;96:592-596.
30. Wicki R, Franz C, Scholl FA, Heizmann CW, Schafer BW. Repression of the candidate tumor suppressor gene S100A2 in breast cancer is mediated by site-specific hypermethylation. *Cell Calcium* 1997;22:243-254.
31. Ebralidze A, Tulchinsky E, Grigorian M, Afanasyeva, A, Senin, V, Revazova E, Lukanidin E. Isolation and characterization of a gene specifically expressed in different metastatic cells and whose deduced gene product has a high degree of homology to a Ca²⁺-binding protein family. *Genes Dev* 1989;3:1086-1093.
32. Barraclough R, Rudland PS. The S-100-related calcium-binding protein, p9Ka, and metastasis in rodent and human mammary cells. *Eur J Cancer* 1994;30A:1570-1576.

33. Albertazzi E, Cajone F, Leone BE, Naguib RN, Lakshmi MS, Sherbet GV. Expression of metastasis-associated genes h-*mts1* (S100A4) and nm23 in carcinoma of breast is related to disease progression. *DNA Cell Biol* 1998;17:335-342.
34. Grigorian MS, Tulchinsky EM, Zain S, Ebralidze AK, Kramerov DA., Kriaievska MV, Georgiev GP, Lukanidin EM. The *mts1* gene and control of tumor metastasis. *Gene* 1993;135:229-238.
35. Wilson CA, Ramos L, Villasenor MR, Anders KH, Press MF, Clarke K, Karlan, B, Chen JJ, Scully R, Livingston D. Localization of human BRCA1 and its loss in high-grade, non-inherited breast carcinomas. *Nat Genet* 1999;21:236-240.
36. Moog-Lutz C, Bouillet P, Regnier CH, Tomasetto C, Mattei MG, Chenard MP, Anglard P, Rio MC, Basset P. Comparative expression of the psoriasin (S100A7) and S100C genes in breast carcinoma and co-localization to human chromosome 1q21-q22. *Int J Cancer* 1995;63:297-303.
37. Scully R, Ganesan S, Brown M, De Caprio JA, Cannistra SA, Feunteun J, Schnitt S, Livingston DM. Location of BRCA1 in human breast and ovarian cancer cells (technical comments). *Science* 1996;272:123-124.
38. Chen Y, Chen P-L, Riley DJ, Lee W-H, Allred DC, Osborne CK. Location of BRCA1 in human breast and ovarian cancer cells (technical comments). *Science* 1996;272:125-126.
39. Ishida-Yamamoto A, Takahashi H, Presland RB, Dale BA, Iizuka H. Translocation of profilaggrin N-terminal domain into keratinocyte nuclei with fragmented DNA in normal human skin and loricrin keratoderma. *Lab Invest* 1998;78:1245-1253.
40. Chen Y, Chen CF, Riley DJ, Allred, D. C. Chen, P. L. Von Hoff, D. Osborne, C. K. Lee, W. H. Aberrant subcellular localization of BRCA1 in breast cancer *Science* 1995;270:789-791.
41. Sheng H, Shao J, Williams CS, Pereira, M. A. Taketo, M. M. Oshima, M. Reynolds, A. B. Washington, M. K. DuBois, R. N. Beauchamp, R. D. Nuclear translocation of beta-catenin in hereditary and carcinogen- induced intestinal adenomas. *Carcinogenesis* 1998;19:543-549.
42. Hessian PA, Edgeworth J, Hogg N. MRP-8 and MRP-14, two abundant Ca(2+)-binding proteins of neutrophils and monocytes. *J Leukoc Biol* 1993;53:197-204.
43. Albertazzi E, Cajone F, Lakshmi MS, Sherbet GV. Heat shock modulates the expression of the metastasis associated gene MTS1 and proliferation of murine and human cancer cells. *DNA*

Cell Biol 1998;17:1-7.

44. Yang Q, D OH, Heizmann CW, Marks A. Demonstration of heterodimer formation between S100B and S100A6 in the yeast two-hybrid system and human melanoma. *Exp Cell Res* 1999;246:501-509.

45. Mandinova A, Atar D, Schafer BW, Spiess M, Aebi U, Heizmann CW. Distinct subcellular localization of calcium binding S100 proteins in human smooth muscle cells and their relocation in response to rises in intracellular calcium. *J Cell Sci* 1998;111:2043-2054.

Figure 1

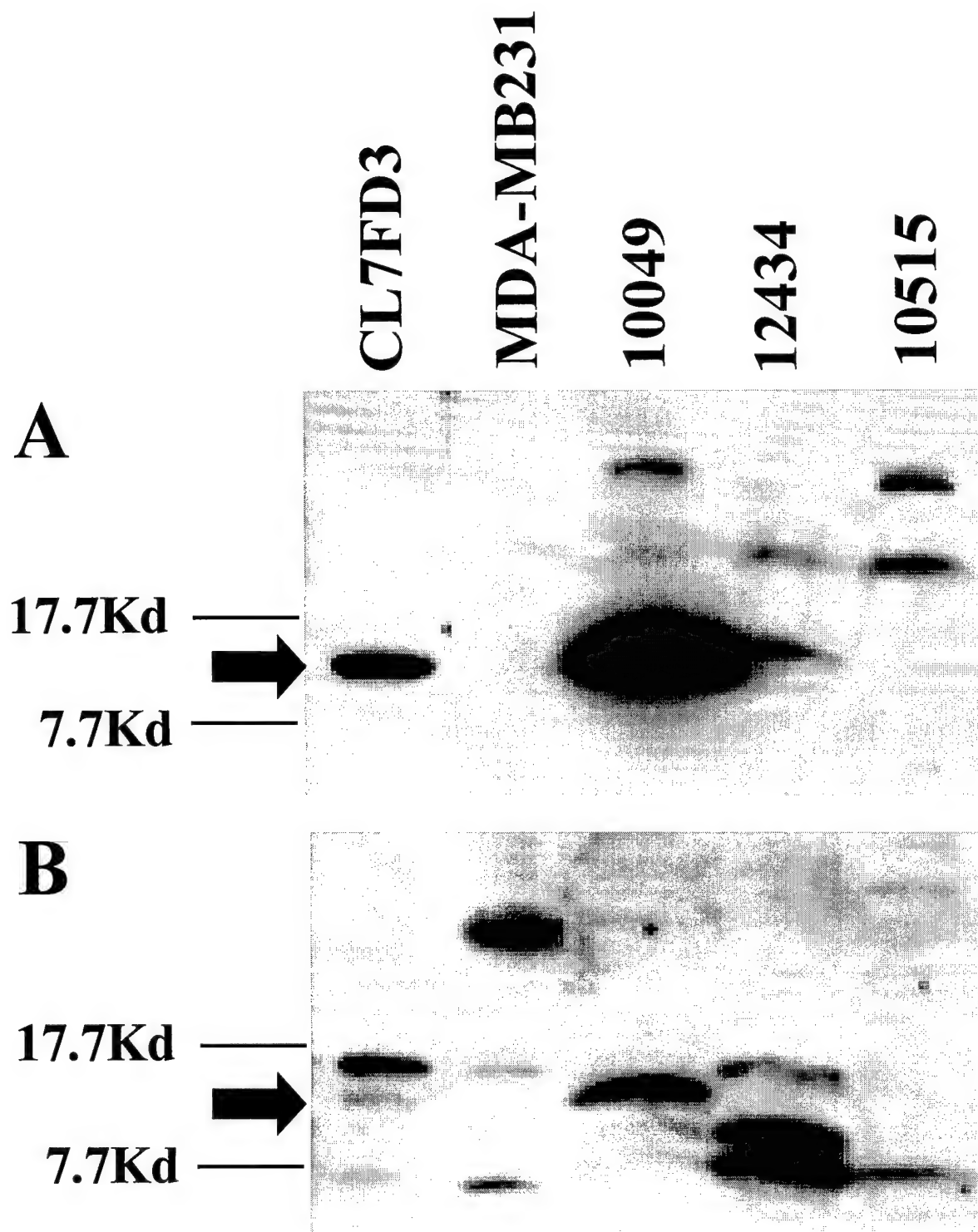
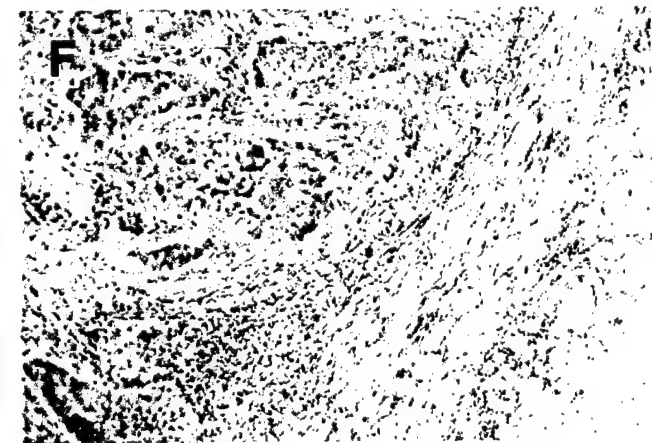
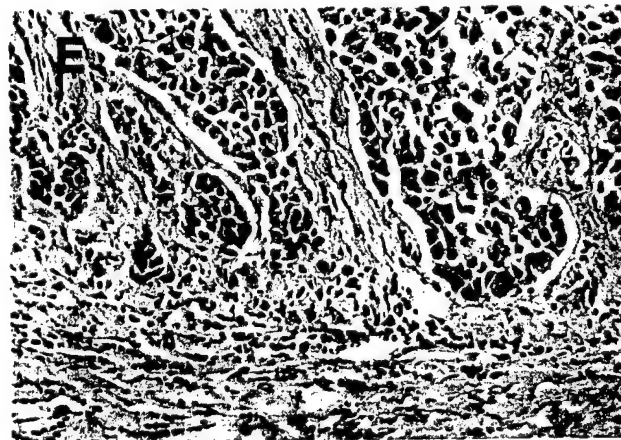
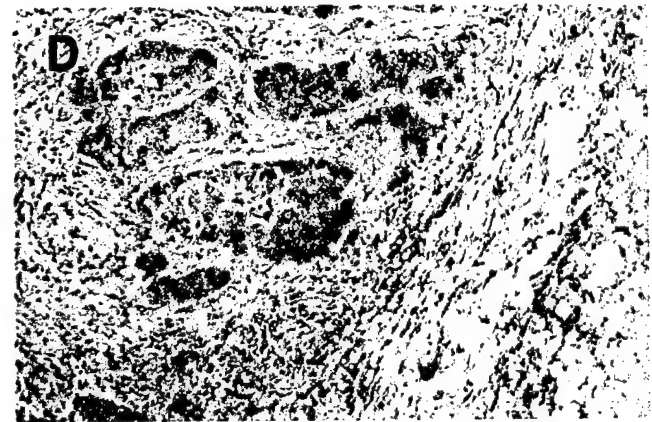
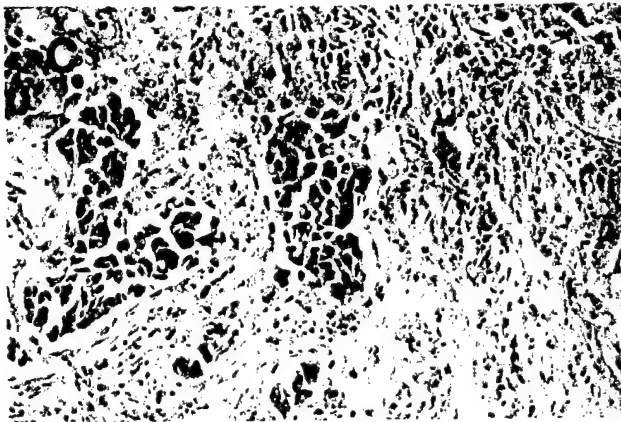


Figure 2



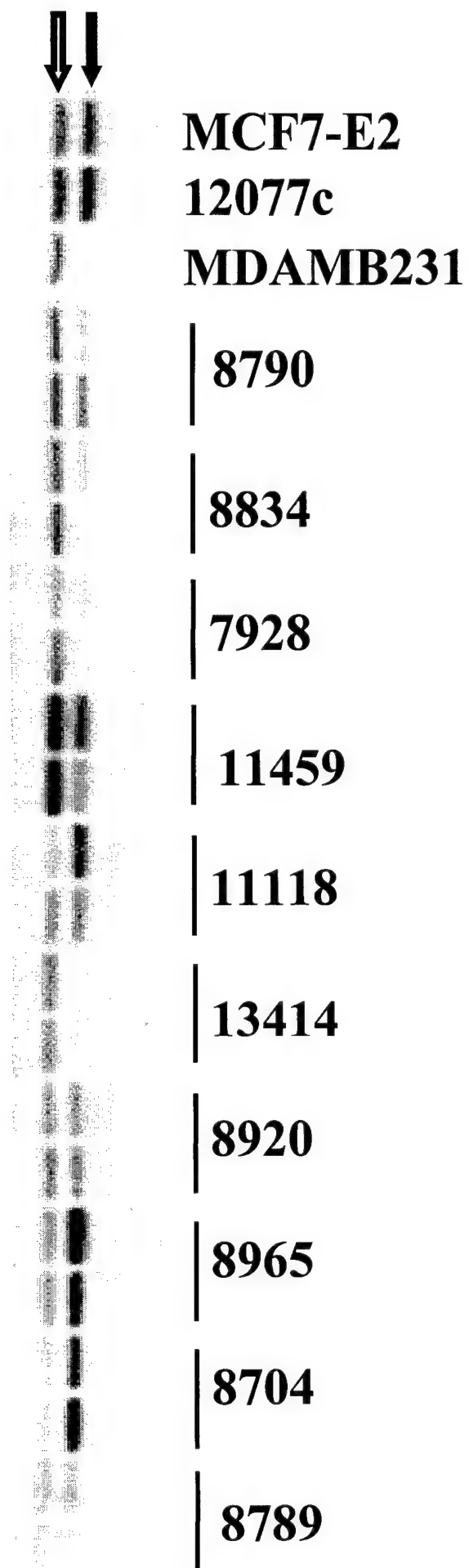


Figure 3

32Kd
17.7Kd
7.7Kd



8021

8814

8789

8993

8674

8799

CL7FD3

MDAMB231

9631

8830

8921

7928

8840

8639

Table 1

TB #	RT-PCR	ISH			IHC		
		int	prop	ISH score	int	prop	IHC score
13402	0.07	0.1	1	0.1	0	0	0
11971	0.13	0.1	1	0.1	0	0	0
8684	0.14	0.5	1	0.5	0	0	0
8840	0.17	0.1	1	0.1	1	0.5	0.5
12037	0.20	0.1	1	0.1	0	0	0
12868	0.21	0.1	1	0.1	0	0	0
10644	0.32	0	0	0	0	0	0
8830	1.06	2	0.1	0.2	1	0.5	0.5
12715	1.24	2	1	2	1	1	1
9631	1.32	1	0.1	0.1	3	1	3
8965	1.85	2	1	2	2	1	2
10049	2.01	2	1	2	2	1	2
8704	2.60	3	0.5	1.5	2	1	2

Table 2

Clinicopathological parameters							Histology					psoriasin		
TB#	type	ER	PR	GrSc	size	NS	Inv%	IS%	N%	Str%	Inf	RT-PCR	RT-PCR/ Inv%	WB
11549	muc	194	133		3	-	40	0	10	50	2	0.06	0.15	-
10515	muc	341	176		3	-	60	0	0	40	1	0.08	0.14	-
9948	muc	46	22		6.5	-	60	0	0	40	1	0.10	0.16	-
10582	muc	109	62		2.3	na	40	0	0	60	1	0.14	0.34	-
8832	muc	295	177		4	-	70	0	0	30	2	1.94	2.77	-
8021	muc	331	328		2.3	-	70	0	0	30	2	0.11	0.15	-
11387	tub	105	35		3.5	na	30	0	0	70	2	0.09	0.29	-
9483	tub	56	0		1.2	-	10	0	0	90	2	0.09	0.91	-
11651	tub	67	24		2.2	-	30	0	0	70	3	0.23	0.77	-
8814	tub	232	103		2	-	30	0	10	60	2	0.44	1.45	-
8720	tub	29	73		2	-	10	0	5	85	1	0.52	5.21	-
12072	tub	8.3	5		2.3	+	50	0	0	50	3	0.67	1.34	-
13041	med	3.4	9		2	-	80	0	0	20	5	0.40	0.49	-
13153	med	4.9	2.4		3	na	80	0	0	20	5	0.61	0.76	-
11867	med	1.4	9		1.6	+	60	0	0	40	5	1.60	2.67	+
13058	med	4.6	12		2.8	-	80	0	0	20	5	1.63	2.04	-
12434	med	1	1.3		1.2	-	50	0	0	50	5	1.63	3.27	+
8639	ilc	52	83		na	-	30	0	20	50	1	0.20	0.67	-
8799	ilc	111	139		6	+	10	0	0	90	2	0.31	3.15	-
8993	ilc	142	528		8	+	60	0	0	40	1	0.52	0.86	-
9801	ilc	2.1	9.8		na	-	35	0	5	60	3	0.56	1.60	-
8921	ilc	2.3	8.9		8	-	50	5	5	40	2	2.07	3.77	+
8961	ilc	0.7	3.4		2.5	-	40	0	10	50	3	2.34	5.84	+
9000	idc	392	596	7	2.5	-	70	0	0	30	1	0.07	0.09	-
13402	idc	49	35	4	2.8	-	40	5	0	55	2	0.07	0.17	-
11971	idc	97	25	4	1.5	-	30	0	10	60	2	0.13	0.42	-
8684	idc	74	43	7	5	+	40	0	0	60	1	0.14	0.35	-
12853	idc	17.3	83	9	4.8	+	70	0	0	30	4	0.15	0.22	-
8840	idc	74	68	7	1.8	+	40	5	0	55	3	0.17	0.37	-
8834	idc	10	147	5	2	-	50	0	5	45	2	0.17	0.34	-
8674	idc	16.7	4.5	9	na	-	55	0	0	45	2	0.19	0.35	-
12037	idc	225	144	4	3.5	+	50	0	5	45	2	0.20	0.40	-
12868	idc	93	141	9	3.5	na	75	0	0	25	1	0.21	0.28	-
8599	idc	58	81	4	3.5	-	30	0	0	70	1	0.24	0.79	-
10105	idc	0.9	3.8	9	3	+	60	0	0	40	4	0.24	0.40	-
7928	idc	33	72	5	3	+	40	0	0	60	2	0.27	0.67	-
13414	idc	15.5	59	5	4.1	-	50	0	0	50	2	0.28	0.56	-
11343	idc	78	44	4	na	-	40	0	10	50	3	0.29	0.73	-
10644	idc	130	4.7	9	3.2	+	40	0	0	60	2	0.32	0.81	-
10137	idc	42	26	7	1.8	-	50	0	0	50	1	0.44	0.89	-
10064	idc	0.8	4.6	9	2.5	na	60	0	0	40	2	0.53	0.88	-
11769	idc	1.1	3.5	7	na	-	70	0	0	30	3	0.56	0.80	-
8932	idc	114	27	4	2	-	50	0	0	50	1	0.56	1.13	-
10906	idc	46	6.6	9	4.5	na	90	0	0	10	5	0.58	0.64	-
8789	idc	0.8	0.4	7	na	na	40	0	0	60	3	0.66	1.64	-
10150	idc	70	42	7	na	-	40	0	0	60	1	0.67	1.68	-
11459	idc	3.6	98	5	4.6	+	70	0	0	30	3	0.67	0.96	-
13191	idc	17.2	9.2	9	3.2	-	80	0	0	20	2	0.69	0.87	-
10124	idc	1.9	12.9	9	3	-	70	0	0	30	4	1.00	1.42	-
8830	idc	0.7	8	9	6	+	80	0	0	20	4	1.06	1.32	+
8790	idc	6	50	5	1.5	+	30	0	0	70	2	1.07	3.58	-
11118	idc	6.6	11.8	5	8.5	+	50	0	0	50	2	1.10	2.20	-
12715	idc	1.5	16	7	3	na	60	0	0	40	3	1.24	2.06	+
9631	idc	0.7	4.5	9	na	+	40	5	5	50	4	1.32	3.10	+
8965	idc	0.4	9.9	7	na	+	70	0	0	30	4	1.85	2.64	+
10049	idc	0.8	14	9	3.7	+	40	0	0	60	4	2.01	5.04	+
8704	idc	0.7	3.5	7	3.5	+	35	5	0	60	2	2.60	6.50	+

Table 3

		ALL				IDC			
		n	low Ps	High Ps		n	low Ps	High Ps	
ER	-	28	14	4	p=0.0001	19	10	9	p=0.0019
	+	29	28	1		15	15	0	
PR	-	25	13	12	p=0.001	15	8	7	p=0.018
	+	32	29	3		19	17	2	
NS	-	30	24	6	ns (p=0.095)	14	13	1	p=0.0002
	+	19	11	8		15	8	7	
INFL	low	34	29	5	p=0.049	20	17	3	ns (p=0.07)
	high	18	11	7		14	8	6	
SIZE	<2	12	9	3	ns	6	5	1	ns
	2 - 5	29	22	7		18	14	4	
	>=5	7	4	3		3	1	2	
GRADE	low					12	10	2	ns
	mod					10	7	3	
	high					12	8	4	
TYPE	Idc	34	25	9	ns				
	Ilc	6	4	2					
	med	5	2	3					
	muc	6	5	1					
	tub	6	6	0					

APPENDIX F

LUMICAN AND DECORIN ARE DIFFERENTIALLY EXPRESSED IN HUMAN BREAST CARCINOMA

Etienne Leygue, Linda Snell, Helmut Dotzlaw, Kate Hole, Tamara Hiller-Hitchcock,
Leigh C. Murphy, Peter J. Roughley, Peter H. Watson ².

Affiliations of authors: Department of Pathology (L. S., K. H., T. H-H., P. H. W.) and Department of Biochemistry and Molecular Biology (E. L., H. D., L. C. M.), University of Manitoba, Faculty of Medicine, Winnipeg, Manitoba, Canada, R3E OW3. Genetics Unit, Shriners Hospital for Children, Montreal, Quebec, Canada, H3G 1A6 (P. J. R.).

Running title: Lumican expression in breast cancer.

Footnotes:

1 This work was supported by grants from the Medical Research Council of Canada (MRC) and the U.S. Army Medical Research and Materiel Command (USAMRMC). The Manitoba Breast Tumor Bank is supported by funding from the National Cancer Institute of Canada (NCIC). P. H. W. is an MRC Scientist, L. C. M. is an MRC Scientist, E. L. is a recipient of a USAMRMC Postdoctoral Fellowship. T. H-H is a recipient of an MRC studentship award.

2 To whom requests for reprints should be addressed, at Department of Pathology, D212-770 Bannatyne Ave, University of Manitoba, Winnipeg, MB. R3E OW3, Canada. Phone: (204) 789 3435; Fax: (204) 789 3931; E-mail: pwatson@cc.umanitoba.ca.

3 The abbreviations used are: SLRP, small leucine rich proteoglycan; RT-PCR, reverse transcription-polymerase chain reaction; H&E, Hematoxylin/Eosin; ER, estrogen receptor; PR, progesterone receptor; PAGE, polyacrylamide gel electrophoresis; PCR, polymerase chain reaction; GAPDH, glyceraldehyde-3-phosphate dehydrogenase. NS = not significant.

Summary

We have previously shown that lumican is expressed and increased in the stroma of breast tumors. We have now examined lumican expression relative to other members of the small leucine-rich proteoglycan gene family in normal and neoplastic breast tissues to begin to determine its role in breast tumor progression. Western blot study showed that lumican protein is highly abundant relative to decorin, while biglycan and fibromodulin are only detected occasionally in breast tissues (n=15 cases). Further analysis of lumican and decorin expression performed in matched normal and tumor tissues by in-situ hybridization showed that both mRNA's were expressed by similar fibroblast-like cells adjacent to epithelium. However, lumican mRNA expression was significantly increased in tumors (n=34, $p<0.0001$) while decorin mRNA was decreased ($p=0.0002$) in neoplastic relative to adjacent normal stroma. This was accompanied by a significant increase in lumican protein (n=12, $p=0.0122$) but not decorin. Further evidence of altered lumican expression in breast cancer was manifested by discordance between lumican mRNA and protein localization in some regions of tumors but not normal tissues. We conclude that lumican is the most abundant of these proteoglycans in breast tumors and that lumican and decorin are inversely regulated in association with breast tumorigenesis.

Key words: Lumican, decorin, small leucine-rich proteoglycan, breast cancer, tumor progression.

Introduction

The development and progression of breast carcinoma is caused by alterations in the expression of multiple genes, most of which are responsible for normal physiological pathways and the necessary cellular interactions to support these functions within the mammary gland. These include alterations in the interactions between the epithelial and stromal cells, which are manifested in tumors by well recognized morphological changes known as the stromal reaction ¹. The influence of such alterations in stromal-epithelial interactions may influence the risk of transformation of the breast epithelial cell and very early steps in tumorigenesis, as has been recently proposed in other systems ². However, the net effects of these alterations in the stroma on later stages of tumor progression is unresolved ³.

Resolution of this issue is complicated by the recognition that the stroma is a highly complex tissue that includes a variety of different types of fibroblasts ⁴ and a range of proteins, glycoproteins and proteoglycans which may play a role in tumor biology. We have recently extended this list by identifying lumican, a member of the small leucine-rich proteoglycans (SLRP's) as an mRNA that is expressed in the stroma of normal breast tissues and overexpressed in invasive carcinomas ⁵. Members of this family of proteoglycans have been implicated principally in matrix assembly and structure ⁶, but also more recently in control of cell growth ⁷. While studies of decorin have shown altered expression in neoplastic stroma ³, lumican has previously been studied only in the context of connective tissue and corneal disease ^{8,9}, and the role of SLRP's in human breast cancer is relatively unexplored. To explore further the potential role of lumican and related genes in breast tumor progression, we have now examined the expression of lumican relative to that of other members of the SLRP family, decorin, biglycan and fibromodulin, at both mRNA and protein level in normal and neoplastic breast tissues.

Materials and methods

Human breast tissues

All breast tumor cases used for this study were selected from the NCIC-Manitoba Breast Tumor Bank (Winnipeg, Manitoba, Canada). As has been previously described¹⁰, tissues are accrued to the Bank from cases at multiple centers within Manitoba, rapidly collected and processed to create matched formalin-fixed-embedded and frozen tissue blocks with the mirror image surfaces oriented by colored inks. The histology and cellular composition of every sample in the Bank is interpreted in Hematoxylin/Eosin (H&E) stained sections from the face of the former tissue block.

For the initial study to broadly compare expression of different members of the SLRP gene family a mixed pilot cohort was selected from the Tumor Bank to include 9 different invasive carcinomas, 3 normal tissue samples from patients with cancer and 3 normal tissues from normal patients without cancer. The invasive tumors included different tumor types (5 ductal, 3 lobular and 1 tubular carcinoma), grades (4 high, 1 moderate, 4 low grade) and estrogen receptor levels (3 ER <10 fmol/mg, 3 ER 10-20, 3 ER 39-169) and total stromal fractions ranging from 50-95% of the cross sectional area. The mean patient ages were 62, 70 and 28 years for each subgroup respectively (tumor tissues, normal tissues adjacent to tumors, normal tissues).

For the subsequent studies to compare lumican and decorin expression a second more defined and homogeneous cohort of 46 cases was selected to prove matching primary tumor tissues and adjacent normal tissue. This cohort included only invasive ductal carcinomas and was primarily selected to ensure availability of histologically confirmed and distinct regions comprising normal and tumor tissue elements in different blocks (12 cases, for Western blot studies) or the same block (34 cases, for in-situ hybridization studies). The subset used for Western blot studies was also selected to possess equivalent cross sectional areas (mean section area^(sd) in tumor tissues = $0.86^{(0.44)}$ cm², adjacent normal tissues = $0.85^{(0.35)}$ cm²) and stromal content (mean stromal area^(sd) in tumor tissues = $68^{(10)}$ %, adjacent normal tissues = $89^{(6)}$ %) between the matching blocks and to incorporate cancer cases from both post-

menopausal patients (6 cases mean^(sd) = 76⁽⁷⁾ years) and pre-menopausal patients (6 cases mean^(sd) = 44⁽³⁾ years) .

Sodium dodecyl sulfate/polyacrylamide gel electrophoresis (SDS/PAGE) and immunoblotting

Total proteins were extracted from frozen tissue sections. These were cut from the face of frozen tissue blocks immediately adjacent to the face of a matching paraffin block ¹¹ from which paraffin sections had been previously cut for pathological assessment and for in-situ hybridization. For the first cohort of cases, an average of twenty 20 micron tissue sections were cut from each typical tissue block (0.5 x 1.0 cm² cross sectional area) and used for extraction, however the number of tissue sections was varied for each case according to the measured area of the tissue within individual blocks to ensure that equivalent volumes of tissue were used for the extraction, which was done as described previously ¹². For the second cohort of matching tissue samples, the same number of frozen sections (twenty x 20 micron) was cut from the measured surface of each tissue block together with a single section from the adjacent paraffin block to be used as a reference for composition, and protein extraction performed on the frozen sections with equivalent volumes of extraction buffer. Proteins present in equivalent volumes of extracts were analyzed by SDS/PAGE and immunoblotting, using anti-peptide antibodies specific for the carboxyl-terminal regions of lumican, decorin, fibromodulin and biglycan ^{9,12}. Protein signals were detected by chemiluminescence and photographed prior to quantitation by video-image analysis and densitometry using an MC M4 software (Imaging Research, St Catherines Ont.). All signals were then adjusted with reference to control cartilage samples run with each blot. For the second cohort of matched tissue samples signals were also adjusted with reference to the measured cross sectional area and the stromal content of the tissue block to control for equivalent loading. Additional analysis was performed on all signals after further adjustment for relative stromal content of the tissue sections assessed in adjacent H&E sections.

Immunohistochemistry

Immunohistochemistry was performed on paraffin sections using the same antibody to lumican as used for immunoblotting. Sections (5 micron thick) were obtained from paraffin embedded tissue blocks matching the frozen tissue blocks of those cases used for RT/PCR and protein analysis. After de-paraffinizing, clearing and hydrating in TBS buffer (Tris Buffered Saline, pH 7.6) the sections were pre-treated with hydrogen peroxide, 3% for 10 minutes to remove endogenous peroxidases and non-specific binding was blocked with normal swine serum 1:10 (Vector Laboratories S-4000). Tris buffered saline (TBS) was used between steps to rinse and as a diluent. Primary antibody to lumican was applied at a 1:400 dilution overnight at 4 °C followed by biotinylated secondary swine anti-rabbit IgG, 1:200 (DAKO) for 1 hour at room temperature (R.T.). Tissue sections were incubated 45 minutes at R.T. with an avidin/biotin horseradish peroxidase system (Vectastain ABC Elite, Vector Lab.) followed by detection with DAB (diaminobenzidine), counterstaining with Methyl Green, 2% and mounting. A positive tissue control (colon mucosa) and a negative reagent control (no primary antibody) were run in parallel. Immunostaining pattern and intensity was assessed by light microscopic visualization.

In-situ hybridization

Paraffin embedded 5 micron sections of breast tissues were analysed by 'in situ' hybridization according to a previously described protocol ⁵. For lumican, the plasmid Lumi-398, that consisted of pGEM-T plasmid (Pharmacia Biotech), containing a 398bp portion of lumican cDNA, between bases 1332 and 1729 was used as a template to generate UTP^{S35} labelled sense and antisense riboprobes using Riboprobe Systems (Promega, Madison, WI.) and either the T7 or SP6 promotor at the 5' or 3' end of the lumican sequence according to the manufacturer's instructions. For decorin, the plasmid Dec-322 was used as a template. This consisted of pGEM-T plasmid containing a decorin insert with a comparable length (322bp) to the lumican probe generated by PCR amplification from the decorin cDNA ¹² using primers that corresponded to decorin (sense 5'-AAATGCCCAAACCTCTTCAG -3' and antisense 5'- AAACCTCAATCCCAACTTAGCC-3') ¹³. All PCR cDNA's and plasmid

inserts were sequenced to confirm their entity. Levels of lumican and decorin expression were assessed in normal and tumor regions by microscopic examination at low power magnification and with reference to the negative sense and positive control tumor sections. This was done as previously described ⁵ by scoring the estimated average signal intensity (on a scale of 0 to 3) and the proportion of stromal cells showing a positive signal (0, none, 0.1, less than one tenth; 0.5, less than one half; 1.0 greater than one half). The intensity and proportion scores were then multiplied to give an overall score. Regions with a score lower than 1.0 were deemed negative or weakly positive.

Microdissection and protein extraction analysis

To assess protein localization within regions of tumors, 2 cases were selected that showed marked and well defined regions within the same tissue section with discrepancies between mRNA and protein expression. This was determined by in-situ hybridization and immunohistochemistry in adjacent serial sections from paraffin tissue blocks. The mirror image frozen tissue blocks to these paraffin blocks were used for microdissection as previously described ¹¹ and protein was extracted from these histologically defined regions as described above. Briefly, thin 5 micron frozen sections were cut from the face of the frozen tissue blocks and stained by H&E, and the relevant histological regions of approximately 1-2 mm ² distinguished and confirmed by reference to the paraffin sections already studied. Multiple thick frozen sections (20 x 20 micron) were then cut, rapidly stained and microdissected at room temperature from each section in turn, and the microdissected tissue fragments frozen again prior to protein extraction.

Results

Identification of lumican as the most abundant SLRP in normal and neoplastic breast tissues

To determine the relative importance of altered lumican expression in breast tumorigenesis the expression of lumican protein was compared to that of three other members of the SLRP family, decorin, fibromodulin and biglycan by Western blot in a heterogeneous panel of 9 breast tumors and 6 normal tissues.

Lumican was highly abundant in all samples and in both neoplastic and normal tissues (Figure 1). A significant increase was seen in the mean level of lumican protein between normal and tumor (mean^(sd) tissue adjusted optical density units, normal = 0.43^(0.08), tumor = 0.56^(0.15), $p = 0.026$, Mann Whitney test). Although an apparent difference in level of lumican between normal samples from normal patients and normal samples adjacent to tumors was seen, this difference did not persist when different stromal content of these samples was taken into account. Nevertheless, an increase in overall molecular weight and polydiversity was noted in normal tissues from older patients relative to younger patients.

In comparison decorin, although also present in most samples examined by Western blot, was much less abundant relative to the cartilage control (Figure 1). It should be noted that the decorin (in common with biglycan and fibromodulin) signals shown in figure 1 also required a 3 fold longer chemiluminescent exposure time (9 seconds) than that for lumican (3 seconds). However in contrast to lumican, there was a marked decrease in decorin between normal and tumor samples (mean^(sd) optical density units; normal = 0.21^(0.06), tumor = 0.13^(0.14), $p = 0.066$, Mann Whitney test). No difference was seen in signals between normal samples from normal and cancer patients.

Fibromodulin expression was not detected in normal tissues and at only low levels in only 3/9 tumors, where the presence of fibromodulin correlated with those tumors with the highest content of epithelial tumor cells. Biglycan was also only detected at low levels in 2/6 normal tissues and 3/9 tumors, where in contrast to fibromodulin its presence correlated directly with those tumors with the highest content of collagenous stroma.

Lumican and decorin are differentially expressed between normal and neoplastic tissues.

In order to examine further the distinct alterations in the expression of lumican and decorin, the mRNA and protein expression of both genes was examined in 46 cases by in-situ hybridization (34 cases) and Western blot (12 cases) from the second cohort of cases, comprising matched normal and tumor samples.

As previously shown, prominent lumican mRNA expression was detected using an antisense probe, in stromal fibroblast like cells within the tumor and immediately adjacent to invasive tumor cells. Assessment of mRNA levels using a semi-quantitative approach as detailed in the Materials and Methods section, also confirmed our previous observations⁵ made on a different set of tumors, and lumican mRNA was found to be significantly elevated in the majority of tumors when levels were compared to those present in adjacent normal stroma ($p < 0.0001$, Wilcoxon test, Figure 2 and 3B). Higher levels of lumican (≥ 1) were present in tumor compared to normal tissue in 26/34 cases. At the same time, decorin levels also showed a consistent and significant difference, with lower levels seen in stroma associated with tumor relative to stroma associated with adjacent normal tissue components ($p < 0.0002$, Wilcoxon test, Figure 2 and 3C), with lower levels of decorin (≥ 1) present in tumor compared to normal tissue in 22/34 cases. The pattern of expression of decorin was also identical in sections from the same cases studied with a different in-situ hybridization riboprobe (data not shown).

In keeping with the pattern of mRNA expression, the mean lumican protein signal assessed by Western Blot was also higher in 9/12 tumors relative to normal tissues (mean^(sd) optical density units, normal = $0.22^{(0.15)}$, tumor = $0.43^{(0.19)}$, $p = 0.0122$ Wilcoxon test). Once again, in contrast to this, decorin protein was lower in 7/12 tumors relative to normal tissues but in this case the differences were not statistically significant (mean^(sd) optical density units, normal = $0.22^{(0.19)}$, tumor = $0.17^{(0.2)}$, $p = \text{ns}$, Wilcoxon test). These contrasting patterns of lumican and decorin expression also persisted after standardisation of Western blot signals for relative stromal content (data not shown).

Lumican mRNA and protein expression can occur in different regions within breast tumors

Immunohistochemical study of lumican distribution within the same tissues that had already been examined by in-situ hybridization was performed using the same antibody that had been employed for Western blot analysis (Figure 4). This showed that lumican was abundant throughout the collagenous stroma of both normal and tumor sections with prominent deposition around small vessels, breast duct and lobular structures. There was increased deposition within the collagenous stroma of tumors, in particular at the invasive margins and in areas of dense collagen within central regions of some tumors, compared to adjacent normal tissues. However, in some cases there were distinct regions, up to 2 mm in area within the tumor sections containing loose stroma in which there was a complete absence of lumican detectable by immunohistochemistry (Figure 4 C&D). However, the same regions showed high expression when examined for lumican mRNA by in-situ hybridization in adjacent sections (Figure 4A&B). Similarly, other areas showed strong staining for lumican protein but low levels of mRNA.

To explore the possibility that the absence of lumican expression detected by immunohistochemistry might be due to the conformation of the native protein or the binding of lumican to other proteins, resulting in the masking of the carboxy-terminal epitope, specific areas measuring approximately 1 mm² each were microdissected from frozen sections of 2 tumors and lumican protein assessed under denaturing conditions by SDS/PAGE and Western blot. In both cases, those regions with high mRNA expression and negative by immunohistochemistry were also negative by Western blot, while areas showing very low mRNA expression but strong staining by immunohistochemistry were positive by Western blot (Figure 5).

Discussion

We have shown that lumican is the most abundant proteoglycan in comparison with several other members of the family of small leucine-rich proteoglycans (SLRP's) in breast cancer. We have also extended our previous observations ⁵, based on the detection of lumican mRNA, in showing that the total lumican protein is also increased in breast tumors relative to adjacent normal tissues. Our results also demonstrate that this pattern of upregulation of lumican in relation to breast tumorigenesis is distinct from that of the closely related decorin gene, which is inversely regulated and reduced at mRNA and to a lesser extent at protein levels, in tumor relative to adjacent normal tissue. Finally, we have shown that lumican expression in tumors may also be associated with abnormal distribution within the stroma manifested by discordance between mRNA and protein deposition within subregions of breast tumors.

The family of SLRP's share several common features, including a central region of leucine rich repeats bounded by flanking cysteine residues and localization in the extracellular matrix. The SLRP's can be separated into three subgroups that include decorin and biglycan, lumican and fibromodulin, epiphykan and osteoglycin, that are distinguishable both by amino acid homologies and also gene structure ¹⁴. Decorin, probably the best studied of these genes, is known to interact with a variety of extracellular matrix molecules and has been shown to be capable of influencing collagen fibril growth and assembly both in-vitro and in-vivo ^{6,15}. Decorin may also influence tumor cell growth through indirect effects on the availability of growth factors from the extracellular matrix or directly through activation of the EGF receptor and induction of the p21 cell cycle inhibitor ¹⁶. In contrast less is known about lumican and other SLRP's. However, in-vitro and in-vivo data indicate that lumican is also important in the regulation of collagen fibril assembly ¹⁷. This view is supported by recent observations based on mice with homozygous deletion of the lumican gene where loss of corneal transparency and increased skin fragility is associated with disorganized and loosely packed collagen fibers related to increased and irregular fibril size, and interfibrillar spacing, as viewed by light and electron microscopy ⁸.

The observation that lumican is highly abundant compared to other SLRP's in breast tumors cannot be interpreted to mean that it is necessarily the most important. This is underscored by the recent demonstration that although decorin is apparently more abundant than versican in prostate cancer tissue, only increase in the larger chondroitin sulphate proteoglycan versican correlates with grade and inversely with progression-free survival in prostate cancer ¹⁸. Similarly, the increase in lumican seen here in association with breast tumorigenesis may be less important than the parallel decrease in decorin. The implications of these alterations in expression await experiments to determine their functional effects. However, increased lumican expression is associated with several parameters indicative of more biologically aggressive tumors ⁵ indicating that the relative changes in different SLRP expression may have a functional effect on tumor progression. It is possible to speculate that both induction of lumican and decrease in decorin in stromal fibroblasts within the invasive tumor may represent a positive host response to abrogate the disorganization of collagen within the tumor stroma, encourage macrophage localization ¹⁹, and inhibit the growth of epithelial cancer cells through the increased availability of growth factors inhibitory to breast epithelial cell growth ²⁰. Alternatively, these alterations may represent a negative host response contributing to tumor progression. Increased lumican mRNA expression may reflect a response to locally increased proteolysis or altered deposition of the lumican protein that is the cause of the disorganization of the collagenous stroma, that in turn facilitates tumor cell invasion. Similarly, a decrease in decorin may remove an inhibitory effect on epithelial tumor cell growth through repression of p21 ⁷. A role for and the distinction between these opposing potential effects will clearly require further study.

The differences in lumican levels between normal and tumor tissues observed by both immunohistochemistry and Western blot are not as marked as those seen at the level of mRNA expression. While differences in the assays may account for some of this discrepancy, it is clear that it may also be attributable to the discordance that can also exist between lumican mRNA and protein expression detected by in-situ and immunohistochemical techniques respectively, within the same regions of breast tumor stroma. A similar discordance between mRNA and protein expression has been previously observed in the

course of studies on lumican and other large and small proteoglycans in different tissues. For example, in corneal development in the chicken, the mRNA levels for lumican and decorin do not always reflect the rate of synthesis of the corresponding proteins and the efficiency of translation of lumican varies over time ²¹. Similar discordance between aggrecan and versican mRNA and protein has been seen in normal tendon ²², between decorin and biglycan mRNA and protein localization in normal and reactive gastric mucosa ²³, and in regions of cartilage matrix around vascular channels and the growth plates of long bones in normal cartilage ²⁴. In this latter instance, the discordance was attributed to high rate of breakdown and removal at these sites. This conclusion is supported by studies on endothelial cells which show that growth factors such as bFGF can not only increase both biglycan transcription and protein synthesis but also the corresponding rate of proteolysis ²⁵. The absence of protein could also reflect masking of the epitope by conformational changes in the native protein, by changes in post-translational modification or by binding to another protein. Alternatively this could reflect reduced translation, increased breakdown, or failure to bind within the immediate stroma and rapid translocation of the protein to adjacent areas of the tissue. Our microdissection experiments, applied to small regions where lumican mRNA is highly expressed suggest that the corresponding protein is truly absent in these areas and that epitope masking due to conformation or binding proteins is an unlikely explanation for the observation. However it could also be the case that the necessary binding sites are not available in the immature stroma associated with rapid growth of tumors and that this allows translocation of newly synthesized lumican to binding sites in adjacent tissue.

The reciprocal nature of the changes in the expression of lumican and decorin is intriguing. Although definitive characterization of the stromal cell types awaits primary culture studies, direct comparison of in-situ hybridization performed on serial sections suggests that expression of both genes apparently occurs in the same fibroblast-like cells in breast tissue stroma. While lumican has not been previously studied in human tumors, expression of decorin mRNA and proteoglycans incorporating chondroitin sulphate epitopes have been shown to be increased in colon, prostate and basal cell carcinomas ²⁶⁻²⁸. However, similar immunohistochemical studies of breast tumors using monoclonal antibodies raised

against chondroitin sulphate and dermatan sulphate small proteoglycan have shown reduced decorin expression within invasive as compared to surrounding normal stroma ²⁹, consistent with our findings. Decorin and other SLRP's are known to be independently regulated and mutually exclusive ²⁴ and compensatory changes in expression between different SLRP's have been observed ³⁰. However this appears to be usually manifested by genes within subgroups of the SLRP family. At the same time, reciprocal changes in expression between lumican and decorin have not been described in lumican or decorin 'knockout' mice ^{8,15}. The factors that influence altered expression of these genes in breast tumor stroma remain to be elucidated.

In summary, we have shown that lumican is highly abundant relative to decorin, biglycan and fibromodulin in normal and neoplastic breast tissues. We have also shown that increased lumican protein expression and altered regional localization occur in breast tumors and that different and reciprocal alterations in expression occur between lumican and decorin. The functional significance and role of alterations in these stromal proteoglycans in breast tumorigenesis and progression remains to be determined.

Figure Legends.

Figure 1. Immunoblotting study of lumican, decorin, biglycan and fibromodulin protein expression in human breast tumors (lanes 1-9), normal tissues from normal patients (lanes 10-12) and normal tissues adjacent to carcinomas (lanes 13-15). All protein samples were extracted from sets of frozen tissue sections bracketed by sections assessed by H&E stain and light microscopy to confirm content. Chemiluminescent signals for decorin, biglycan and fibromodulin required 3 fold longer exposure times than that for lumican. Molecular markers (left) and cartilage control sample (right) are present in all panels.

Figure 2. Lumican and decorin mRNA levels in matched normal and tumor tissues assessed by in-situ hybridization and semi-quantitative scoring as described in Materials and Methods. The thickness of each line (on a scale of 1 to 9) corresponds to the number of cases showing the same differences in scores (n=34 cases).

Figure 3. Lumican and Decorin mRNA expression detected by in-situ hybridization within a breast tumor section. Panel A (H&E section) shows the histology including the invasive tumor (upper area), the tumor margin (middle) and adjacent normal tissue including lobular-ductal units (lower area). Lumican expression (panel B) is high within the tumor and tumor margin and lower in the normal fat and collagenous stroma adjacent to the normal lobules. Decorin (panel C) shows high expression in the normal stroma adjacent to normal lobules and reduced expression in the tumor. Original magnification x400.

Figure 4. In-situ hybridization and immunohistochemical study showing regional discordance in lumican mRNA (panels A & B) and protein expression (panels C & D) displayed in adjacent sections in breast tumors. Panels A and C show overall pattern of mRNA (A, black signal) and protein (C, brown staining) within a tissue section (0.4 x 0.8 cms in size) that includes regions of in-situ and invasive tumor (upper left and upper middle) and adjacent normal tissue (lower left and lower right). Panels B & D show a detailed microscopic view (original magnification x400) of the cellular localization of mRNA and protein within a small

region at the invasive edge within the same section (tumor component at left, normal component at right)

Figure 5. Lumican protein expression detected by immunohistochemistry (upper panel) and Western blot (lower panel) demonstrating concordance in assessment of protein levels in microdissected subregions within two breast tumor sections. The upper panels show IHC sections (tumor A, right; tumor B, left; scale bar = 5mm). The mRNA and protein signals were detected by in-situ hybridization (ISH) and immunohistochemistry (IHC) in each region in adjacent sections and ISH/IHC levels were assessed semi-quantitatively (negative, weak +, strong ++) as follows; tumor A; region 1 = ++/-, region 2 = -/++, region 3 (remainder of section) = +/++; tumor B; region 4 = +/-, region 5 = -/++, region 6 = ++/++. The lower panel shows the Western blot (C = cartilage control, lanes 1-6 correspond to regions assessed and microdissected above).

References

1. Peyrol S et al. Lysyl oxidase gene expression in the stromal reaction to in situ and invasive ductal breast carcinoma. *Am J Pathol* 1997; **150**: 497-507.
2. Kinzler KW, Vogelstein B. Landscaping the cancer terrain [comment]. *Science* 1998; **280** : 1036-7.
3. Iozzo RV. Tumor stroma as a regulator of neoplastic behavior. Agonistic and antagonistic elements embedded in the same connective tissue [editorial]. *Lab Invest* 1995; **73**: 157-60.
4. Spanakis E, Brouty-Boye D. Discrimination of fibroblast subtypes by multivariate analysis of gene expression. *Int J Cancer* 1997; **71**: 402-9.
5. Leygue E et al. Expression of lumican in human breast carcinoma. *Cancer Res* 1998; **58**: 1348-52.
6. Iozzo RV. The family of the small leucine-rich proteoglycans: key regulators of matrix assembly and cellular growth. *Crit Rev Biochem Mol Biol* 1997; **32**: 141-74.
7. Santra M et al. Ectopic expression of decorin protein core causes a generalized growth suppression in neoplastic cells of various histogenetic origin and requires endogenous p21, an inhibitor of cyclin-dependent kinases. *J Clin Invest* 1997; **100**: 149-57.
8. Chakravarti S et al. Lumican regulates collagen fibril assembly: skin fragility and corneal opacity in the absence of lumican. *J Cell Biol* 1998; **141**: 1277-86.
9. Cs-Szabo G, Melching LI, Roughley PJ, Glant TT. Changes in messenger RNA and protein levels of proteoglycans and link protein in human osteoarthritic cartilage samples. *Arthritis Rheum* 1997; **40**: 1037-45.
10. Watson PH, Snell L, Parisien M. The NCIC-Manitoba Breast Tumor Bank: a resource for applied cancer research. *Cmaj* 1996; **155**: 281-3.
11. Hiller T, Snell L, Watson PH. Microdissection RT-PCR analysis of gene expression in pathologically defined frozen tissue sections. *Biotechniques* 1996; **21**: 38-40.
12. Grover J, Chen XN, Korenberg JR, Roughley PJ. The human lumican gene. Organization, chromosomal location, and expression in articular cartilage. *J Biol Chem* 1995; **270**: 21942-9.
13. Vetter U, Vogel W, Just W, Young MF, Fisher LW. Human decorin gene: intron-exon junctions and chromosomal localization. *Genomics* 1993; **15**: 161-8.
14. Hocking AM, Shinomura T, McQuillan DJ. Leucine-rich repeat glycoproteins of the extracellular matrix. *Matrix Biol* 1998; **17**: 1-19.
15. Danielson KG et al. Targeted disruption of decorin leads to abnormal collagen fibril morphology and skin fragility. *J Cell Biol* 1997; **136**: 729-43.
16. Moscatello DK et al. Decorin suppresses tumor cell growth by activating the epidermal growth factor receptor. *J Clin Invest* 1998; **101**: 406-12.
17. Ying S et al. Characterization and expression of the mouse lumican gene. *J Biol Chem* 1997; **272**: 30306-13.

18. Ricciardelli C et al. Elevated levels of versican but not decorin predict disease progression in early-stage prostate cancer. *Clin Cancer Res* 1998; **4**: 963-71.
19. Funderburgh JL et al. Macrophage receptors for lumican. A corneal keratan sulfate proteoglycan. *Invest Ophthalmol Vis Sci* 1997; **38**: 1159-67.
20. Santra M, Skorski T, Calabretta B, Lattime EC, Iozzo RV. De novo decorin gene expression suppresses the malignant phenotype in human colon cancer cells. *Proc Natl Acad Sci U S A* 1995; **92**: 7016-20.
21. Cornuet PK, Blochberger TC, Hassell JR. Molecular polymorphism of lumican during corneal development. *Invest Ophthalmol Vis Sci* 1994; **35**: 870-7.
22. Waggett AD, Ralphs JR, Kwan AP, Woodnutt D, Benjamin M. Characterization of collagens and proteoglycans at the insertion of the human Achilles tendon. *Matrix Biol* 1998; **16**: 457-70.
23. Schonherr E, Luger N, Stoll R, Domschke W, Kresse H. Differences in decorin and biglycan expression in patients with gastric ulcer healing. *Scand J Gastroenterol* 1997; **32**: 785-90.
24. Bianco P, Fisher LW, Young MF, Termine JD, Robey PG. Expression and localization of the two small proteoglycans biglycan and decorin in developing human skeletal and non-skeletal tissues. *J Histochem Cytochem* 1990; **38**: 1549-63.
25. Kinsella MG, Tsoi CK, Jarvelainen HT, Wight TN. Selective expression and processing of biglycan during migration of bovine aortic endothelial cells. The role of endogenous basic fibroblast growth factor. *J Biol Chem* 1997; **272**: 318-25.
26. Adany R, Heimer R, Caterson B, Sorrell JM, Iozzo RV. Altered expression of chondroitin sulfate proteoglycan in the stroma of human colon carcinoma. Hypomethylation of PG-40 gene correlates with increased PG-40 content and mRNA levels. *J Biol Chem* 1990; **265**: 11389-96.
27. Hunzelmann N et al. Altered immunohistochemical expression of small proteoglycans in the tumor tissue and stroma of basal cell carcinoma. *J Invest Dermatol* 1995; **104**: 509-13.
28. Iozzo RV, Cohen I. Altered proteoglycan gene expression and the tumor stroma. *Experientia* 1993; **49**: 447-55.
29. Nara Y et al. Immunohistochemical localization of extracellular matrix components in human breast tumours with special reference to PG-M/versican. *Histochem J* 1997; **29**: 21-30.
30. Nelimarkka L et al. Expression of small extracellular chondroitin/dermatan sulfate proteoglycans is differentially regulated in human endothelial cells. *J Biol Chem* 1997; **272**: 12730-7.

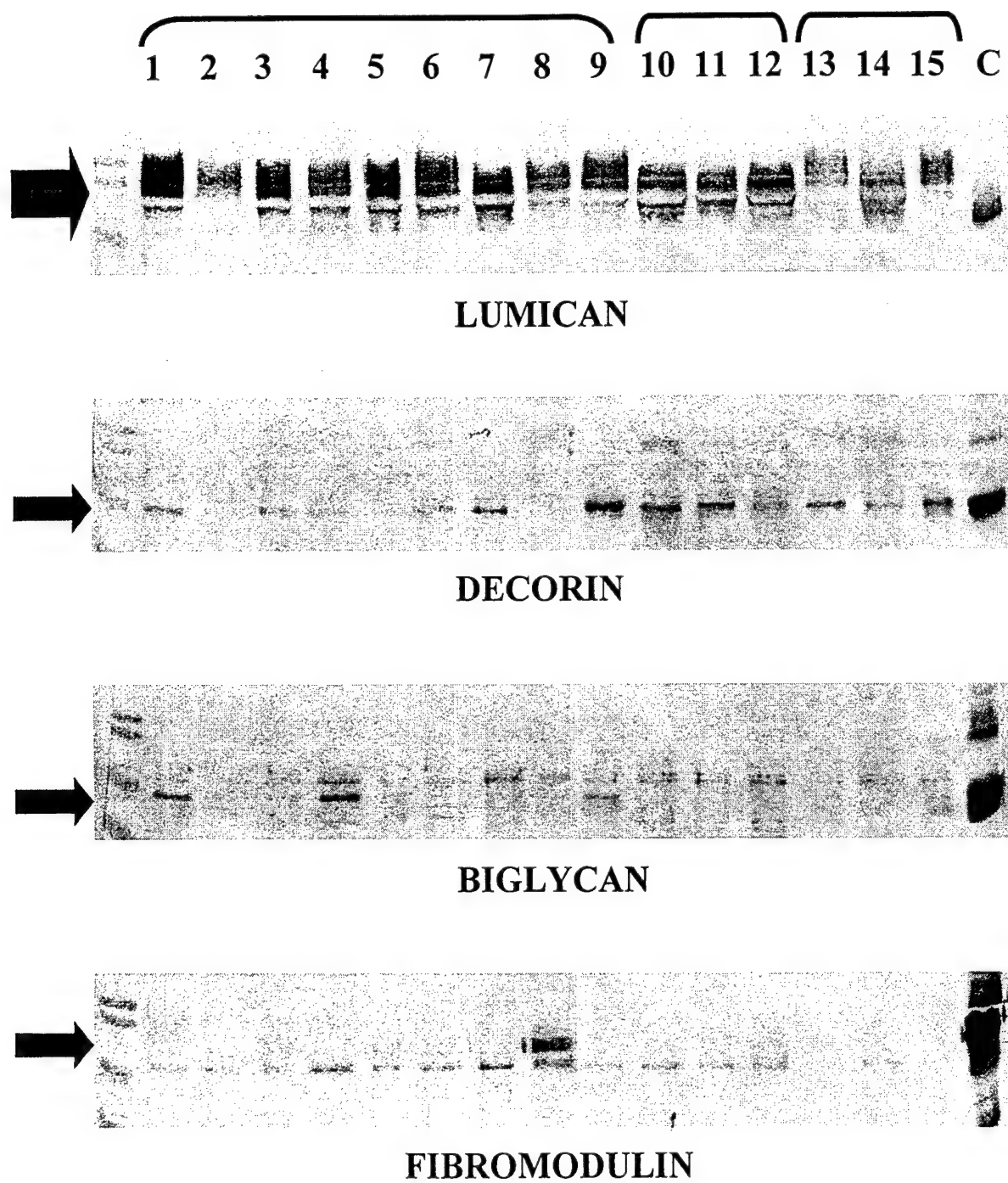
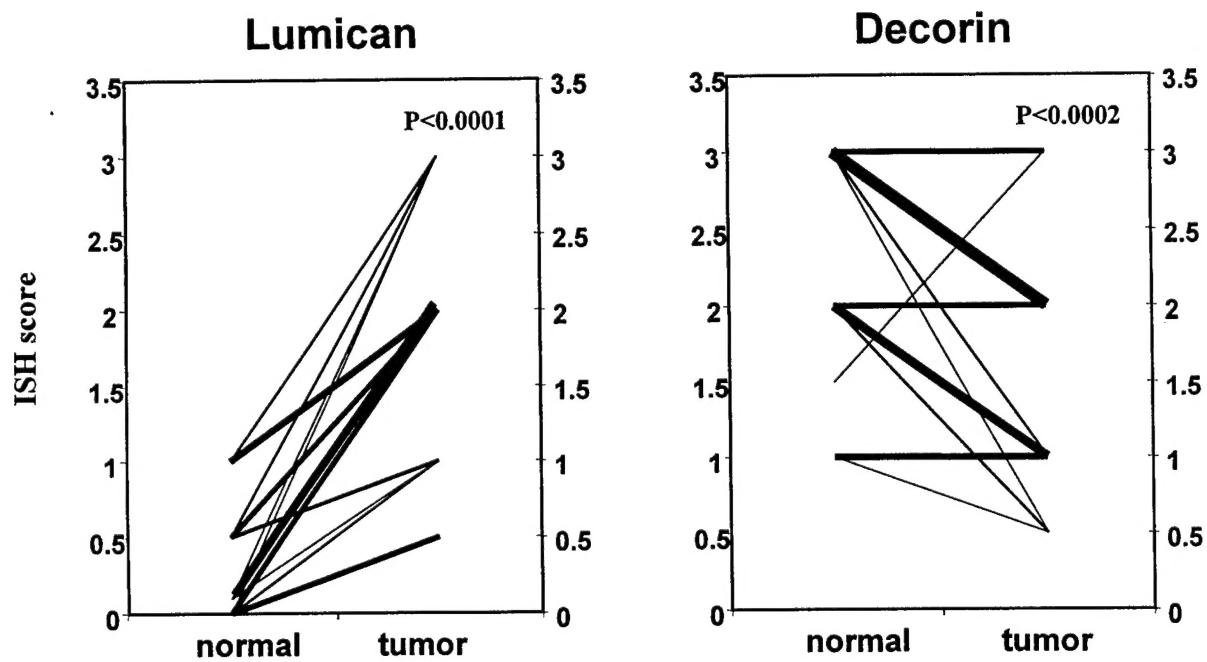


Figure 2



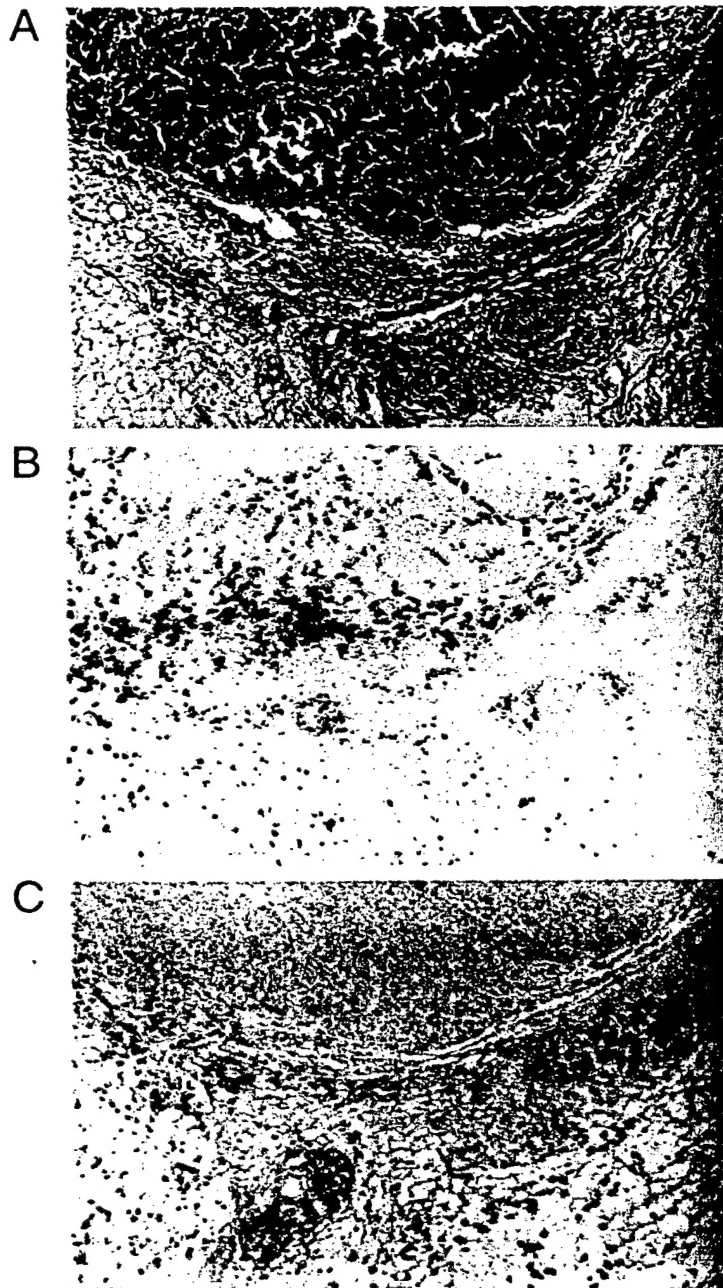


Figure 4



B



D



A



C

Fig 4

2

2

Figure 5

